5

Single-Molecule FRET: Methods and Biological Applications

Ling Chin Hwang, Johannes Hohlbein, Seamus J. Holden, and Achillefs N. Kapanidis

Abstract Since the first single-molecule fluorescence resonance energy transfer (FRET) measurement in 1996, the technique has contributed substantially to our understanding of biological molecules and processes by probing the structure and dynamics of nucleic acids, protein molecules, and their complexes with other molecules. This review discusses basic concepts and current developments in single-molecule FRET methodology, as well as examples of applications to systems such as nucleic acid machines and molecular motors.

5.1. Introduction

Probing molecular structure, dynamics, and interactions at the 1- to 10-nm scale is central to our understanding of the molecules responsible for the myriad of fascinating processes occurring each minute in living cells. The special interest in this length scale arises from the simple fact that most of the proteins, nucleic acids, and lipids that form the structures, sensors, gates, and machines in the cell have nanometre-scale dimensions. For example, double-stranded DNA has a diameter of 2 nm; haemoglobin has a diameter of ∼6 nm; and the lipid bilayer of a cell membrane is ∼5 nm thick. Ever since it was realized that diffraction poses a fundamental limit in the direct visualisation of biomolecules using conventional optical microscopy, researchers have recruited various ingenious ways to break the diffraction barrier and access the all-important nanometre scale. A celebrated member in the category of such methods is based on the phenomenon of fluorescence resonance energy transfer (FRET), also known as Förster resonance energy transfer in honor of Theodor Förster, who in 1948 developed the main FRET theory. Since its first demonstration as a molecular ruler (Stryer and Haugland 1967), FRET has been used extensively at the levels of both molecular ensembles and single molecules and has been an instructive method in both *in vitro* and *in vivo* settings. FRET is not only a tool for basic science studies, but also has sparked several important applications. For example, clever designs in fluorophore combinations for FRET enabled faster and cheaper sequencing of the human genome. In addition, several bioassays used in the biotechnology industry are based on the concept of FRET. In this review, we provide a

L. C. Hwang, J. Hohlbein, S. J. Holden, and A. N. Kapanidis • Department of Physics and IRC in Bionanotechnology, Clarendon Laboratory, University of Oxford, Oxford, OX1 3PU, UK

short introduction on FRET and discuss fundamentals of single-molecule FRET along with selected applications on biological and bio-inspired systems. For further reading, readers are also encouraged to consult other excellent reviews on ensemble FRET (Clegg 1992; Selvin 1995; Selvin 2000) and single-molecule FRET (Ha 2001; Ha 2004; Schuler and Eaton 2008; Weiss 1999; Weiss 2000).

5.2. FRET Fundamentals and Ensemble FRET

FRET is a distance-dependent, non-radiative energy transfer process that occurs between a fluorophore and a chromophore as a consequence of long-range dipole–dipole coupling (Förster 1948); in most cases, the chromophore is also a fluorophore, and the probes are introduced in a single biomolecule or a complex of biomolecules. After excitation of the high-energy fluorophore (donor, D; Figure 5.1A,C) via an external light source, the energy can be transferred to a low-energy fluorophore (acceptor, A) as long as two preconditions are fulfilled: first, both fluorophores are in close proximity (<10 nm); and second, the emission
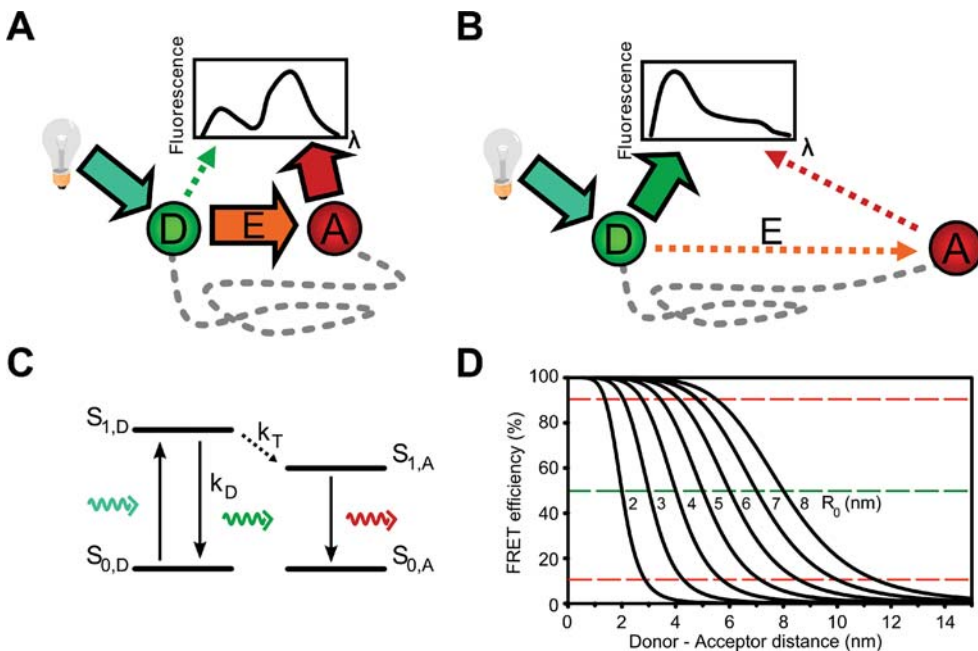
Figure 5.1. Principles of fluorescence resonance energy transfer (FRET). **A.** A light source directly excites the donor dye molecule (*green*). As long as the acceptor dye (*red*) is in close proximity, the energy can be transferred non-radiatively from the donor to the acceptor, resulting in increased emission intensity. **B.** If the distance between the donor and the acceptor is increased, the fraction of transferred energy decreases, resulting in increased emission intensity in the part of the spectrum corresponding to the donor emission wavelength. **C.** Simplified Jablonski diagram showing the transition pathways occurring in the energy transfer process. After excitation of the donor dye into its first excited singlet state, two processes can occur: the donor system can either relax to its ground state by emitting a green photon with a rate constant k_D, or the energy can be transferred to the acceptor molecule with a rate constant of k_T. In the latter case, the acceptor relaxes by emitting a red photon. Other electronic transitions, such as bleaching and intersystem crossing, are neglected. **D.** The FRET efficiency strongly depends on the Förster radius R_0 and is plotted as a function of the donor-to-acceptor distance and R_0.

spectrum of the donor overlaps with the absorption spectrum of the acceptor. As a consequence of energy transfer, the emission intensity of the donor decreases ("donor quenching") and the emission intensity of the acceptor increases ("acceptor sensitization").

The FRET process is often represented by a simplified Jablonski diagram (named after Polish physicist Aleksander Jabłoński) (Figure 5.1C), which is a free-energy state diagram that illustrates the electronic states of the fluorophores and the transitions between them. After excitation of the donor ($S_{0,D} \rightarrow S_{1,D}$), the donor can relax to its ground state $S_{0,D}$ either by emitting a photon or by losing energy as heat. In the presence of an acceptor in close proximity, the donor can also transfer its energy non-radiatively to the first excited singlet state $S_{1,A}$ of the acceptor. The FRET efficiency E between the two excited states $S_{1,D} \rightarrow S_{1,A}$ (Lakowicz 2006) is given by Eq. 5.1, where k_D the fluorescence emission rate constant of the donor in the absence of the acceptor and k_T, the energy transfer rate constant. According to Förster, E is inversely proportional to the sixth power of the distance R between the two fluorophores,

$$E = \frac{k_T}{k_T + k_D} = \frac{1}{1 + (R/R_0)^6} \tag{5.1}$$

The Förster radius R_0, which describes the donor-to-acceptor distance where the FRET efficiency equals 50%, takes values between 2 and 7 nm (Selvin 2000) for common pairs of fluorophores and can be calculated using

$$R_0^6 = \frac{9000(\ln 10)\Phi_D \kappa^2}{128\pi^5 N n^4} \int_0^\infty f_D(\lambda)\varepsilon_A(\lambda)\lambda^4 d\lambda \tag{5.2}$$

where Φ_D is the donor quantum yield in the absence of the acceptor, κ^2 is the orientation factor, N is Avogadro's number, and n is the refractive index of the intervening solution. The overlap integral of the donor emission spectrum and the acceptor absorption spectrum is calculated as a function of the wavelength λ using $\varepsilon_A(\lambda)$ as the molar extinction coefficient of the acceptor and $f_D(s)$ as the normalized emission spectrum of the donor, $\left(\int f_D(\lambda)d\lambda = 1\right)$. The orientation factor κ^2 describes the orientation of the emission dipole of the donor with respect to the absorption dipole of the acceptor and is often a matter of debate (Dale et al. 1979; Haas et al. 1978; Wu and Brand 1992). The factor κ^2 can take values between 0 (for perpendicular dipoles) and 4 (for collinear dipoles). In the limiting case of unrestricted rotational freedom of the dyes, averaging about all possible relative orientations yields $\kappa^2 = 2/3$ (Dale et al. 1979). Rotational freedom can be assessed by measuring fluorescence anisotropy, the change in polarisation between excitation and emission light. For polarised excitation, anisotropy is defined as:

$$r = \frac{I_\perp - I_\parallel}{I_\perp + 2I_\parallel} \tag{5.3}$$

where $I_\parallel$ is the emission intensity parallel to excitation, and $I_\perp$ is the emission intensity perpendicular to excitation. For cases of low anisotropy, the rotational freedom is high and the corresponding assumption of $\kappa^2 = 2/3$ is likely to be valid. For the less common case of high anisotropy, the rotational freedom of at least one fluorophore is likely to be restricted and therefore the uncertainty on R_0 and any associated distances will increase; the uncertainty increases further if both fluorophores have restricted rotational freedom.

The FRET efficiency can be determined in many ways (Clegg 1992; Jares-Erijman and Jovin 2003). Often, the FRET efficiency is measured using the decrease in the fluorescence

emission intensity of the donor or the "FRET-sensitized" emission intensity of the acceptor. Moreover, the equation $\tau^{-1} = k_D + k_T = \tau_D^{-1} + k_T$, which relates the rate constants in Eq. 5.1, to the fluorescence lifetime (τ is the donor fluorescence lifetime in the presence of the acceptor, and τ_D is the donor fluorescence lifetime in the absence of the acceptor) provides another means for determining the FRET efficiency according to

$$E = 1 - \frac{\tau}{\tau_D} \tag{5.4}$$

The $1/R^6$ dependence of the energy transfer on the donor-to-acceptor distance was experimentally verified in classic experiments by Haugland and Stryer in 1967 in which oligomers of poly-L-proline were used as spacers between the donor and the acceptor (Stryer and Haugland 1967); additional experiments using double-stranded DNA as a standard provided further validation (Clegg et al. 1993). Such studies established FRET as a type of "spectroscopic ruler", in that its use offers the intriguing possibility of determining the distance between the fluorophores by measuring the FRET efficiency between fluorophores and calculating the distance R_0 for the fluorophore pair used. During the last 30 years, FRET has become a widely used method on the ensemble level, with many applications on biomolecular structure and dynamics, especially with regards to proteins, nucleic acids, and protein–nucleic acid complexes. FRET between different variants of the green-fluorescence protein (GFP) has also been used extensively for testing for the presence of specific protein–protein interactions in living cells (Lippincott-Schwartz et al. 2001; Miyawaki and Tsien 2000; Zimmer 2002). Ensemble FRET has been extensively reviewed in many excellent reviews covering a broad range of applications (Clegg 1992; Clegg 1995; Jares-Erijman and Jovin 2003; Selvin 1995; Selvin 2000; Wu and Brand 1994). An extensive overview of different fluorophores for FRET can also be found in Sapsford et al. 2006.

Ensemble FRET measurements can provide much insight into the molecular world of biology. However, since ensemble methods report on the mean properties of populations of billions of molecules (e.g., a 16-μL solution of 10 nM DNA contains 1 billion DNA molecules), sample heterogeneity can skew the mean properties to a degree that complicates or even thwarts the interpretation of experiments. This is especially true in cases of large, unstable, or dynamic biomolecules such as protein–nucleic acid complexes or unfolded proteins. For instance, an ensemble of proteins in solution is composed of proteins in either their native state or a denatured state. In the latter case, the mean end-to-end distance of the N-terminus and the C-terminus increases. If both ends are labeled with a donor and an acceptor, respectively, it is clear that an ensemble FRET measurement will reveal only an averaged FRET efficiency with limited access to the different subpopulations (Haas et al. 1975). Ensemble methods are also limited by their inability to monitor stochastic (and, thus, unsynchronizable) dynamic motions, especially under equilibrium conditions. Such motions produce "dynamic heterogeneity", defined as the presence of molecular conformations in which a single molecule or molecular complex dwells for a measurable time during the timescale of observation.

5.3. Single-Molecule FRET Methods Based on Single-Laser Excitation

Some of the shortcomings of ensemble FRET were overcome by single-molecule FRET, which is essentially the observation of FRET at the level of single molecules (Figure 5.2). To achieve this high sensitivity, one needs to use dilute samples in which
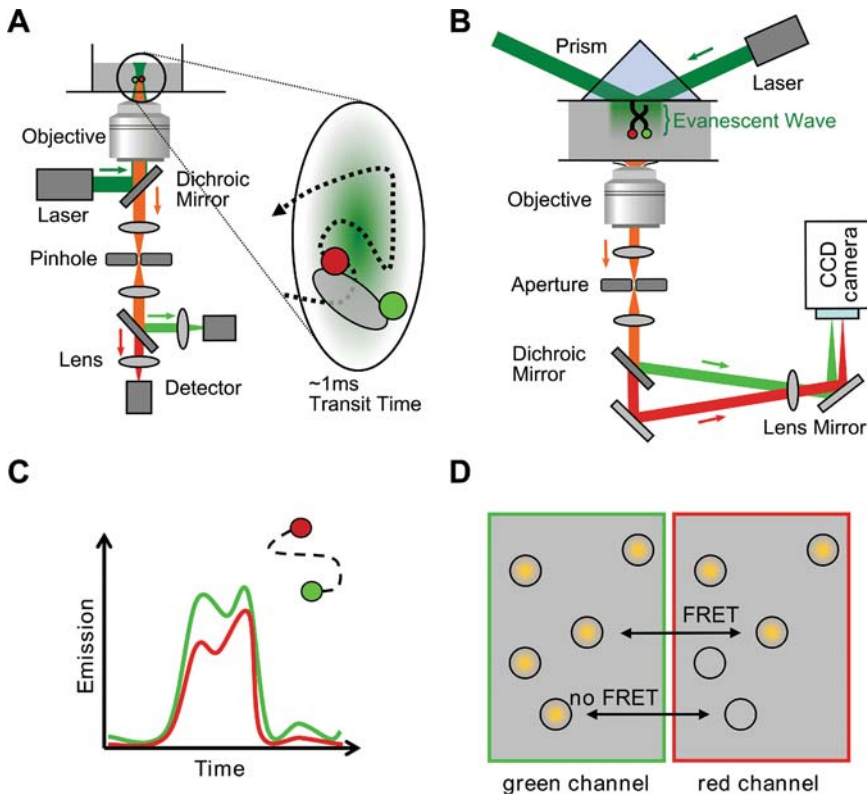
Figure 5.2. Instrumentation for single-molecule fluorescence resonance energy transfer (FRET). **A, B.** Simplified confocal microscopy setup for FRET detection of single molecules diffusing in solution and a setup for total internal reflection fluorescence (prism type) for imaging single molecules immobilised on a cover slide surface. Whereas in the confocal mode the avalanche photodiodes (APDs) act as point detectors of a diffraction-limited spot in the solution, the charge-coupled device (CCD) images color-separated molecules directly. **C.** A typical time trace obtainable for confocal detection in solution. If a molecule enters the focus with a donor and an acceptor attached to it, the detectable intensity in the green and the red detection channels increases. **D.** Immobilized molecules on a surface. If the molecule of interest is only labeled with a donor, no fluorescence will be visible in the red detection channel of the CCD camera.

individual molecules can be resolved; a small excitation/detection volume to reduce the contribution of the background; and bright and photostable fluorophores to achieve a high signal-to-noise ratio. All these features were included in the first successful detection of single-molecule FRET, reported in a pioneering paper by Ha et al. (1996). Near-field scanning optical microscopy (NSOM; a form of scanning probe microscopy that employs evanescent fields emerging from metal-coated fiber tips to probe fluorescence from immobilised single molecules) (Betzig and Chichester 1993; Betzig and Trautman 1992) was used to create a tiny excitation volume to resolve single-labeled DNA molecules dried on the surface of a microscope coverslip. The FRET efficiency was measured between a single tetramethylrhodamine fluorophore (TMR; acting as donor) and a single Texas red fluorophore (acting as an acceptor) attached to either end of a short, double-stranded DNA (dsDNA) fragment. The fluorescence was recorded either using two avalanche photodiodes (sensitive point detectors) dedicated to the donor-emission and the acceptor-emission channels or by a charge-coupled device (CCD)
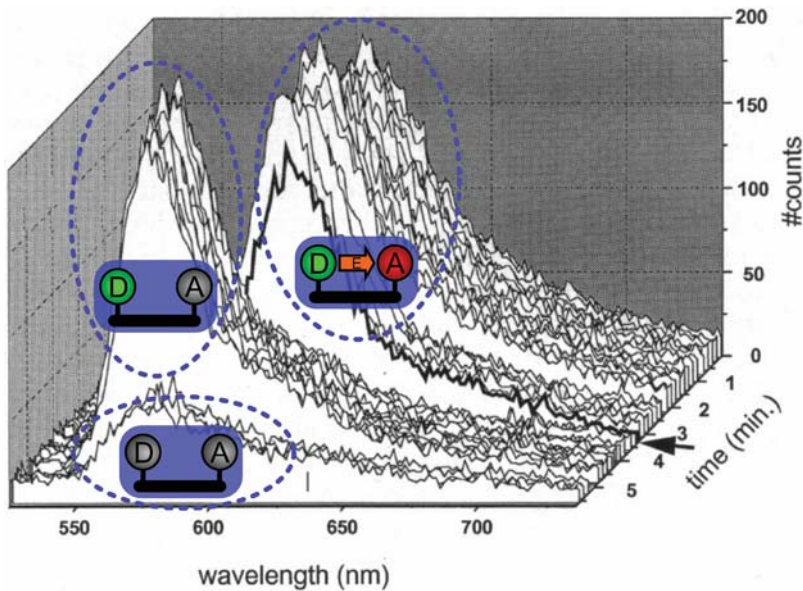
Figure 5.3. Time evolution of emissions during the first single-molecule fluorescence resonance energy transfer (FRET) observation. During the first minutes, the energy of the excited donor is transferred to the acceptor dye. After bleaching of the acceptor (around 3 min of detection), the donor intensity increases because no energy can be transferred to the acceptor. After 5 min the donor bleaches and the intensity is reduced to background levels (due to autofluorescence from the near-field scanning optical microscope tip and possibly fluorescence from distant molecules). See text for details. [Adapted from Ha et al. (1996). Copyright 1996 National Academy of Sciences.]

camera that recorded the emission spectra of individual molecules (Figure 5.3). The detection of single molecules was verified by single-bleaching steps of the fluorophores within the recorded emission spectra. If single molecules are present, the changes in the emission spectra are abrupt and represent either the "ON" or the "OFF" state of the donor and the acceptor, respectively. If, for example, the acceptor is photobleached and thereby becomes fluorescently inactive, the donor emission intensity increases and the acceptor emission vanishes. If the donor bleaches before the acceptor, both emission intensities decrease to the background level. Both cases allow the calculation of FRET efficiencies by using the integrated fluorescence intensities of the donor and acceptor. However, despite the superior resolution of NSOM compared to wide-field confocal microscopy, the NSOM approach requires sophisticated sample scanning and accurate positioning relative to the probed molecules to ensure effective excitation by the evanescent field. Moreover, the metallic tip may influence the emission properties of the fluorophores (Ambrose et al. 1994). Finally, such a method can only probe the surface of biological samples (such as cell membranes).

During this first demonstration of single-molecule FRET (smFRET), and, in general, in most single-excitation smFRET experiments (Figure 5.2A–C), one collects photons emitted in the donor- and acceptor-emission channels upon donor excitation for a smFRET pair under observation; we define these photon counts as $f_{D_{exc}}^{D_{em}}$ and $f_{D_{exc}}^{A_{em}}$, where $f_{D_{ex}}^{D_{em}}$ is the photon count for D-excitation-based D-emission and $f_{D_{ex}}^{A_{em}}$ is the photon count for D-excitation-based A-emission. The extent of FRET can be evaluated using a convenient expression of FRET efficiency, E^* (which does not account for spectral cross-talk in the acceptor-emission channel):

$$E^* = \frac{f_{D_{ex}}^{A_{em}}}{f_{D_{ex}}^{A_{em}} + \gamma f_{D_{ex}}^{D_{em}}} \tag{5.5}$$

Here γ is a detection-correction factor that depends on the donor and acceptor quantum yields and the detection efficiencies of the donor and acceptor emission channels; typically $0.5 < \gamma < 2$. A simpler expression that can still observe relative FRET changes assumes $\gamma = 1$; in that case, one recovers a *proximity ratio*, E_{PR}:

$$E_{PR} = \frac{f_{D_{ex}}^{A_{em}}}{f_{D_{ex}}^{A_{em}} + f_{D_{ex}}^{D_{em}}} \tag{5.6}$$

Where accurate FRET values are required (e.g., for evaluating donor–acceptor distances within biomolecular complexes), it is necessary to measure cross-talk and detection-correction factors (see Section 5.5.1).

In 1999, Ha et al. presented the first studies using a confocal microscope to observe temporal fluctuations of FRET at single-molecule level as a result of protein conformational changes. This study initiated a move from near-field to far-field excitation, which is the current standard for smFRET. It also marked a transition from studies in air to studies in biological buffers, which is necessary for relating smFRET results to the work from ensemble biochemical and biophysical experiments. The conformational changes in this study were modulated by ligand binding, which altered the rotational dynamics and the distances between the conjugated dyes (Ha et al. 1999b). A similar confocal microscope was also used to track conformational changes of individual three-helix-junction RNA molecules and changes induced by either RNA-binding proteins or Mg^{2+} (Ha et al. 1999c).

The use of confocal microscopy for single-molecule detection (Nie et al. 1994) with its high signal-to-noise ratio paved the way for the detection of single-molecule FRET in solution (Deniz et al. 1999). A series of 40-bp-long dsDNA fragments was labeled with a donor at the 5′ end and an acceptor at different positions along the DNA strand. For performing the measurements, a final concentration of ~30 pM was used. Based on the assumption of an excitation/detection volume of a confocal microscope of <1 fL (approximated as a rotational ellipsoid with a short axis of ~400 nm and a long axis of ~2 μm in diameter), the probability of single-molecule occupancy is ~1%, and thereby (following Poissonian statistics) it is several magnitudes larger than the probability of having >1 molecule at the same time within the focus. The paper showed the successful separation of different species within one sample due to the different FRET efficiencies of each species. Moreover, it showed changes in the FRET histograms arise due to DNA cleavage by a DNA-restriction enzyme causing the denaturation of DNA. Besides using intensity ratios for calculating FRET efficiencies, more sophisticated methods of detection and analysis use an array of parameters obtainable from fluorescence detection, such as fluorescence lifetimes and fluorescence anisotropies. This method was developed by Rothwell et al. (2003) to reveal the heterogeneity of HIV-1 reverse transcriptase (see Section 5.7.2).

Using confocal microscopy for the detection of single-molecule FRET has the advantage that the time range for studying dynamics is only limited by the time resolution of the single-point detector (up to nanoseconds). Therefore, confocal microscopy is an attractive tool for sorting molecules and monitoring biomolecular dynamics at the microsecond timescale. However, as a point-detection method, confocal microscopy typically detects only a single molecule at a given time. For parallel detection of multiple molecules, two-dimensional

detectors (e.g., CCD cameras) are necessary, which require the use of wide-field excitation. Two wide-field microscopy methods are commonly used: epifluorescence microscopy and total internal reflection fluorescence (TIRF) microscopy (Moerner and Fromm 2003). In epifluorescence microscopy, the laser excitation light is focused to the back-focal plane of the microscope objective, resulting in an expanded illuminated area that is collinated (Funatsu et al. 1995). In TIRF microscopy (Axelrod 2001), a collinated ray of light in a high–refractive index medium (e.g., glass) hits the interface with a lower–refractive index medium (e.g., water) at an angle larger than the critical angle for total reflection generating an evanescent wave in the second medium. The intensity distribution of the evanescent wave decays exponentially within a few hundred nanometres. For single-molecule detection, two TIRF excitation schemes can be used (Moerner and Fromm 2003). In the objective-type TIRF, the laser light is focused into an extreme edge of the back focal plane of the microscope objective. The prism-type TIRF uses an objective-independent excitation path and consists of a prism optically coupled to a cover glass (Figure 5.2B). In contrast to the epifluorescence wide-field illumination, TIRF excitation has the advantage of a reduced axial excitation volume, leading to lower background, but at the expense of limited time resolution as compared to point detection. The time resolution of ultra-sensitive electron-multiplying CCD cameras is limited to the CCD readout time, which is on the order of few milliseconds.

The first experimental realisation of TIRF-based single-molecule FRET examined the catalysis and folding of individual *Tetrahymena thermophila* ribozyme molecules (Zhuang et al. 2000) (see also Section 5.7.1). The ribozyme was labeled at both ends with a donor and an acceptor, surface-immobilized, and studied using either confocal scanning microscopy or TIRF microscopy. The fluctuations observed between two FRET states demonstrated the folding and unfolding of the ribozyme tertiary structure. Dwell-time analysis of both states produced equilibrium constants that were consistent with ensemble measurements (Zhuang et al. 2000). The studies revealed a rarely populated docked state (with a "fast" folding rate of 1 sec^{-1}), which was not observed using ensemble methods; this rate was discovered on top of the known longer rate of 0.016 sec^{-1} and a misfolded rate of 0.036 hr^{-1}, suggesting an additional folding pathway across a highly rugged energy landscape. Whereas the fast docking kinetics was measured using scanning confocal microscopy, the TIRF detection scheme was used to study the cleavage and overall folding kinetics for several hundred molecules simultaneously. Apart from its biological significance, this groundbreaking work included several aspects that are now the hallmarks of a successful use of a single-molecule technique to address a biological system and question. It was shown convincingly that the attachment of a donor and an acceptor to the large ribozyme does not alter the reaction kinetics of the ribozyme. Moreover, the surface immobilisation of the ribozyme did not affect the single-molecule reaction kinetics when compared to an ensemble kinetic. Finally, the single-molecule results showed directly the presence of distinct states and their dwell time; such complex analysis would simply have been impossible with ensemble measurements.

5.4. Single-Molecule FRET Methods Based on Alternating Laser Excitation

During the last few years, single-molecule FRET methods have been extended to allow direct probing of the FRET acceptor alternating laser excitation (ALEX) (Kapanidis et al. 2004) directly reports on the presence and state of both donor and acceptor fluorophores, by alternately exciting the sample at donor (*D*) and acceptor (*A*) excitation wavelengths.

The donor excitation provides the standard smFRET information, but it is the direct excitation of the acceptor that allows the relative fluorophore stoichiometry to be determined, virtual molecular sorting. ALEX (Figure 5.4D–E) provides smFRET with an additional photon count, for acceptor emission upon *direct* acceptor excitation the fluorescence stoichiometry ratio S (Kapanidis et al. 2004; Lee et al. 2005).

$$S = \frac{f_{D_{ex}}}{f_{D_{ex}} + f_{A_{ex}}} \tag{5.7}$$

The additional information is summarized in a two-dimensional histogram (Figure 5.4F). Sorting can remove artifacts that complicate FRET (such as the presence of states with inactive FRET donor or acceptor and the presence of complex fluorophore stoichiometries) while introducing new observables, such as the observation of an acceptor-only population, which is helpful for evaluating biomolecular interactions.

There are three complementary implementations of ALEX that among them cover a vast range of probe timescales, extending from nanoseconds to hours. Experiments on systems at chemical equilibrium (or systems undergoing kinetic changes occurring on the timescale of a few minutes) can be carried out using solution-based measurements and laser modulation at the microsecond timescale. This approach provides static snapshots of the FRET state of molecules as they diffuse through a femtolitre-size focal volume. This is the most straightforward implementation of the ALEX technique, and it has found numerous applications for measurements of the chemical kinetics of biomolecules (Kapanidis et al. 2005; Kapanidis et al. 2006; Lee et al. 2007).

For nonequilibrium experiments and minute-scale simultaneous observation of dynamics of multiple molecules, one can use the method of millisecond-ALEX (msALEX) (Margeat et al. 2006), which combines TIRF microscopy with laser modulation at the millisecond timescale. msALEX uses TIRF-illumination of surface-immobilised molecules combined with an alternating-laser scheme to carry out subpopulation sorting on surface-immobilised molecules, with the primary advantage over solution measurements of simultaneous observation of multiple smFRET molecules for extended periods of time (seconds to several minutes) (Margeat et al. 2006). One of the main advantages of msALEX over traditional surface smFRET is that by monitoring changes in the stoichiometry parameter S for time traces, it is possible to deconvolve fluctuations in FRET due to distance variations from fluctuations in fluorophore photophysics (such as acceptor blinking) (Margeat et al. 2006; Sabanayagam et al. 2004), a process that has been observed with many popular single-molecule fluorescence probes such as Cy5, tetramethylrhodamine, and Alexa647; blinking significantly increases the uncertainty on single-excitation smFRET measurements. Time traces of S can also report on the kinetics of assembly/disassembly reactions.

To probe fast dynamics and recover fluorescence-lifetime-based observables, one can use the method of nanosecond-ALEX or pulsed interleaved excitation (nsALEX/PIE) (Laurence et al. 2005; Müller et al. 2005), which uses alternation of pulsed laser sources at the nanosecond timescale. The time for a diffusing fluorophore to emit fluorescence after the excitation pulse is recorded and used to carry out fluorescence lifetime analysis in addition to ALEX-based analysis. This allows analysis of fast smFRET distance fluctuations, high-time-resolution fluorescence correlation spectroscopy (FCS), and time-resolved polarisation anisotropy measurements, which may be useful for increasing the accuracy of distance measurements extracted from FRET data (Laurence et al. 2005).

Single-molecule FRET   **Alternating-Laser Excitation**
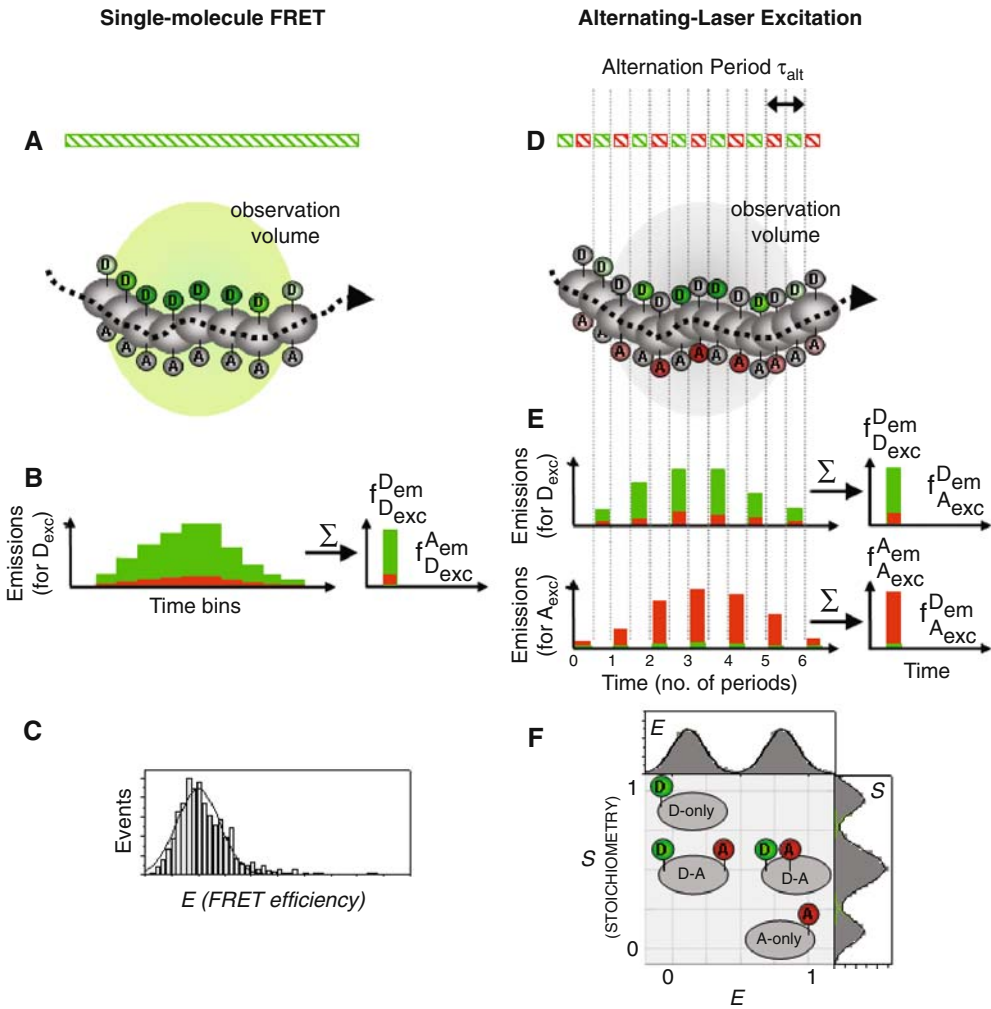
Figure 5.4. Concept of alternating-laser excitation (ALEX) and comparison with single-excitation, single-molecule fluorescence resonance energy transfer (FRET). **A–C.** Single-molecule FRET using single-laser excitation; diffusing-molecule example. A fluorescent molecule transverses a focused green-laser beam and emits photons at the donor- and acceptor-emission wavelengths. The photon counts at these two wavelengths are used to generate one-dimensional histograms of FRET efficiency, E. **D–F.** Single-molecule FRET using alternating-laser excitation. A fluorescent molecule transverses an observation volume illuminated in an alternating fashion using focused green- and red-laser beams. Using the photons emitted in the donor- and acceptor-emission wavelengths for each laser excitation, one can generate a two-dimensional histograms of FRET efficiency E and relative fluorophore stoichiometry S, enabling molecular sorting (see text for details).

5.5. Quantitative Single-Molecule FRET

5.5.1. Measuring Accurate FRET

To obtain *accurate FRET* values rather than proximity ratios, one can measure the contribution of excitation and emission cross-talk terms, the detection efficiency of each detection channel, and the quantum yield of the donor and acceptor fluorophores. The accurate E value is defined as

$$E = \frac{f^{FRET}}{\gamma f^{D_{em}}_{D_{ex}} + f^{FRET}} \tag{5.8}$$

where

$$f^{FRET} = f^{A_{em}}_{D_{ex}} - Lk - Dir \tag{5.9}$$

The terms Lk (donor leakage in the acceptor-detection channel) and Dir (acceptor emission in the acceptor-detection channel due to direct excitation by the donor-excitation laser) describe cross-talk contributions in the $f^{A_{em}}_{D_{ex}}$ signal; such cross-talk terms need to be subtracted from the $f^{A_{em}}_{D_{ex}}$ signal to recover the photon count associated only with FRET [Eq. (5.6)]. The Y term is the detection – correction factor from Eq. (5.5).

For solution-based measurements, these terms are obtained using μsALEX. The factor γ is directly related to the gradient on the E–S histogram of donor-acceptor labeled molecules of varying E, and Lk and Dir are obtained from the donor-only and the acceptor-only subpopulations, respectively. [for details see Lee et al. (2005)].

In the case of immobilised molecules, one follows the methodology of Ha et al. (1999a) or Edel et al. (2007), extracting γ and other correction factors by direct measurement of the change in emitted donor and acceptor intensity upon acceptor photobleaching, determined for individual molecules where the acceptor photobleaches before the donor. This can then be applied for all molecules in the experiment, allowing accurate E values to be obtained.

5.5.2. Obtaining Distances from Single-Molecule FRET Data

Once accurate FRET is obtained, Eq. (5.1) can be used to obtain interprobe distances. The major uncertainty on conversion of E to distances comes from uncertainty in the relative orientation of the smFRET pair, described by the orientation factor κ^2 (see Section 5.2). If κ^2 changes for a given sample (e.g., due to a change in rotational freedom of one of the fluorophores), R_0 will also change, and the distance value obtained will therefore be inaccurate (Dale et al. 1979). This can be addressed by measuring the fluorescence anisotropy (see Section 5.2), which provides a good estimate of the rotational freedom of the fluorophores. Ensemble anisotropy measurements (see Section 5.2) measure the anisotropy averaged over all subpopulations; for many applications, this will be an entirely sufficient check on the rotational freedom. However, ensemble measurements do not entirely address the possibility that rotational freedom is restricted for only some of the sample subpopulations, although in many cases this will still result in a noticeably high ensemble value, which will indicate that rotation is likely to be restricted to some extent. A very useful application of nsALEX/PIE is the ability to directly measure the rotational freedom of both fluorophores at a subpopulation level

(Laurence et al. 2005), thereby better estimating κ^2 and reducing the uncertainty on distance measurements obtained with smFRET.

5.5.3. Triangulation Methods

A promising application of smFRET methods is the use of multiple surface-based FRET measurements to accurately triangulate the position of part of a biomolecule in three dimensions (Andrecka et al. 2008; Rasnik et al. 2004). Multiple FRET-based distance measurements are made between an element with a known crystal structure, such as DNA helicase (Rasnik et al. 2004) or RNA polymerase (RNAP) (Andrecka et al. 2008), and a single point of unknown structure or dynamics (DNA for DNA helicase, mRNA for RNAP). The combination of multiple measurements allows the three-dimensional position of the unknown element to be determined relative to the known structure by simple geometry. In the case of DNA helicase, this provided important information on its DNA-binding orientation; in the case of RNAP, this allowed tracking of the exiting mRNA during transcription elongation. The use of more measurements than the minimum three required for triangulation allows self-consistency checks to be carried out on the measurements, the uncertainty on the measurements, particularly with respect to the orientation factor κ^2 (Rasnik et al. 2004).

5.6. Current Developments in Single-Molecule FRET

5.6.1. Multiple FRET Pair Methods

Single-molecule FRET typically consists of a single two-color donor–acceptor pair. However, a single pair will report only a single distance at a time. To probe several distances simultaneously, adding a third fluorophore is equivalent to performing three two-color experiments. This labeling scheme detects molecular interactions of up to three molecules and adds a third dimension for measuring conformational changes and dynamics of complex biomolecules.

The laboratory of Taekjip Ha was the first to extend three-color FRET to the single-molecule level (Hohng et al. 2004); this was achieved on DNA four-way junctions (see also Section 5.7.1) labeled with a donor (Cy3) and two acceptors (Cy5 and Cy5.5) on three arms of the junction. Three-color smFRET measurements were performed on surface-immobilised junctions using a single 532-nm laser for Cy3 excitation. Three avalanche photodiodes recorded the fluorescence intensities of single DNA molecule in a focused laser spot. By observing correlated intensity changes among three fluorophores, the group was able to probe the well-synchronized movements of two of the acceptor arms to and from the third donor arm and to show that nonparallel conformers of the junctions are dominant. Three-color FRET using a single excitation laser has also been applied to freely diffusing single molecules to simultaneously monitor mixtures of triply labeled (Alexa488, TMR, and Cy5) DNA duplex at multiple distances (Clamme and Deniz 2005).

Use of single-laser donor excitation can pose problems with distinguishing different FRET pathways among the three fluorophores. Moreover, multicolor FRET involves the selection of fluorophores with overlapping donor emission and acceptor excitation spectra, depending on the interprobe distances probed and the R_0 for the different FRET pairs. If

there is large spectral overlap between the dye pairs (such as acceptors, Cy5 and Cy5.5), careful selection or custom-made dichroic mirrors and filters are crucial for separating their signal. Because there is significant cross-talk into the acceptor channels, control experiments have to be conducted to determine their cross-talk and correct for them. To address such challenges and monitor multiple accurate distances without previous information about the molecular structure, Lee et al. (2007) introduced alternating-laser excitation with three-color FRET (3c-ALEX) of diffusing molecules. Using alternating-laser excitation for each of the fluorophores on a triply labeled DNA duplex (Alexa488, TMR, Alexa647), they were able to sort molecules of a single sample measurement into three-dimensional stoichiometry and FRET histograms (Figure 5.5). The stoichiometry histogram identifies the molecules according to their fluorophore stoichiometry, that is, singly, doubly, or triply labeled molecules, independent of FRET efficiency. The FRET histogram depends on the three intermolecular distances of each dye pair, improving the resolution of conformational heterogeneity compared to a one-dimensional FRET histogram. The authors applied 3c-ALEX to study the translocation of *Escherichia coli* RNAP on DNA. They showed that with a single system consisting of a singly labeled RNAP and a DNA doubly labeled at both ends surrounding the start site, there is a concomitant change in the FRET efficiency of the fluorophore pairs arising from the downstream translocation of RNAP on DNA. The method of 3c-ALEX was also used recently to study the structure and folding of a triply labeled 8-17 deoxyribozyme in solution (Lee et al. 2007); the group showed that the deoxyribozyme folds to form a pyramidal structure upon adding Mg^{2+} by monitoring three-color FRET changes with increasing concentrations of Mg^{2+}.

A major challenge for multicolor setups is to have a high signal-to-noise ratio in all detection channels, and this has been limited by tri-band dichroic mirrors with limited transmission wavelengths and broad reflective regions. To improve the signal-to-noise ratio of multicolor ALEX setups, Ross et al. (2007) used a programmable acousto-optical beamsplitter with user-defined wavelengths to achieve the same detection efficiency as single-color setups. Using DNA three-way junctions hybridized on surfaces, the authors resolved seven subpopulations with different stoichiometry, quantified FRET efficiencies in the presence of competing FRET pathways, and observed correlated molecular dynamics.

5.6.2. Combinations of Single-Molecule FRET with Other Single-Molecule Methods

Combining smFRET with methods allowing the manipulation of single molecules by applying external forces opens a new field of exciting applications. A range of such applications was proposed in 1999 by Shimon Weiss in a visionary article (Weiss 1999); among other combinations, methods that combine FRET with patch-clamp, atomic force microscopy (AFM), and optical/magnetic tweezers were suggested. A number of recent reviews also discussed the prospects of combination methods and possible applications (Deniz et al. 2008; Greenleaf et al. 2007; Walter et al. 2008).

The combination of FRET and electrical recording of single-ion channels was shown in 2003 by Borisenko et al. (2003 and Harms et al. (2003); both groups studied the heterodimer formation from gramicidin monomers in a lipid bilayer. Whereas a FRET signal can give information about the distance between differently labeled monomers, the electrical recording allows validation of ion channel formation at the same time.
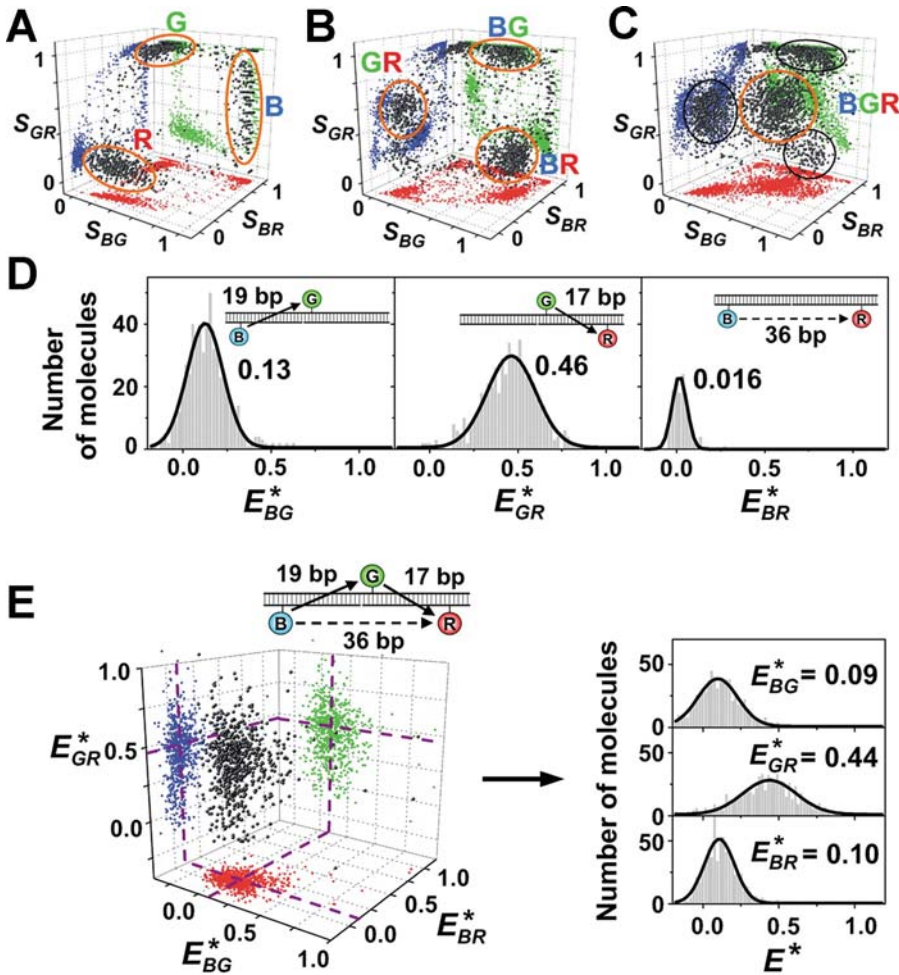
Figure 5.5. Molecule sorting based on probe stoichiometry S. **A.** Three-dimensional S histograms for a 1:1:1 mixture of B-only, G-only, and R-only. **B.** Three-dimensional S histograms for a 1:1:1 mixture of three doubly labeled species (B-G, G-R, and B-R). **C.** Three-dimensional S histograms of triply labeled species (B-G-R). The cluster at the center of the histogram (*orange ovals*) corresponds to B-G-R. Black ovals surround clusters corresponding to the doubly labeled species. **D, E.** Measuring distances within triply labeled and doubly labeled species in the same solution. The reported E^* values represent the means of the fitted Gaussian distributions. Panel D shows the one-dimensional E^* histograms for B-G, G-R, and B-R species, selected from the black circles in panel C. Panel E shows the three-dimensional E^* histograms for the triply labeled species B-G-R, selected from the orange circles in panel C, and the one-dimensional E^* histograms obtained after collapsing the three-dimensional histogram on each of the E^* axes.

An instrument capable of combining FRET with optical trapping was suggested in 2003 by Lang et al. (2003) and was demonstrated experimentally in 2007 by two groups (Hohng et al. 2007; Tarsa et al. 2007). Tarsa et al. (2007) described the use of optical traps mechanically to unzip DNA hairpins by simultaneously monitoring the conformational states of the DNA using FRET, whereas Hohng et al. (2007) extended the method by watching DNA four-way junctions (see also Section 5.7.1), allowing the detection of nanometre-scale motion at sub-pN forces.

Whereas optical traps allow only the translational movement of a loaded bead, magnetic traps can be used to rotate the paramagnetic bead. In addition, using magnetic tweezers prevents photophysical effects that can arise from optical traps. The combination of FRET and magnetic tweezers (Shroff et al. 2005) used a single-stranded DNA oligomer to measure the forces internal to a small DNA loop, showing the possibility of tuning the sensor's force response by using the distances between the dyes.

Single-Molecule FRET in Living Cells

Despite the potential of single-molecule FRET as a noninvasive technique for *in vivo* studies, there have been few *in vivo* single-molecule FRET reports, mainly due to a series of experimental challenges. First, the background autofluorescence from the cell interferes with the detection of fluorescence emission from labeled biomolecules. Second, due to size and labeling requirements, typical fluorophores used in living cells (organic fluorophores and fluorescent proteins) are of moderate brightness and photostability, leading to low signal-to-noise ratio and short photobleaching lifetimes, respectively. Premature bleaching of the fluorophores may lead to misinterpretation of the molecular interactions and dynamics. Semiconductor quantum dots (Michalet et al. 2005)—novel probes displaying tunable emission wavelengths, superior brightness, and longer photobleaching rates—may provide an alternative for *in vivo* labeling; however, quantum dot internalisation and specific targeting to sites or proteins of interest is not trivial. Third, fluorophore labeling methods in living cells can be rather complex and often not as specific (Kapanidis and Weiss 2002).

In vivo applications of smFRET have been limited to cell membrane proteins because these proteins are accessible for fluorescent labeling and molecular interactions. Moreover, fluorescent molecules on membranes can be visualised using TIRF microscopy (see Section 5.2),which does not suffer as much as epifluorescence from out-of-focus background and concomitant decrease in the signal-to-background ratio. Along these lines, one of the first examples of single-molecule FRET examined epidermal growth factor receptor (EGFR) signaling in living cells using objective-type TIRF microscopy equipped with dual-view optics (Sako et al. 2000). The study tracked single molecules of Cy3-labeled epidermal growth factor (EGF) in the plasma membrane of A431 carcinoma cells and observed that EGFR dimers were preformed before the binding of the second EGF molecule; this observation was confirmed by adding a mixture of EGF–Cy3 and EGF–Cy5 and measuring their FRET signal as they colocalized on the membrane (Figure 5.6). The study also used a labeled monoclonal antibody specific to the phosphorylated EGFR (Cy3–mAb74) and Cy3–Cy5 coincidence analysis to show that EGFR becomes phosphorylated after dimerisation; this conclusion was reached by observing the colocalization of Cy3–mAb74 with spots of Cy5–EGF with double the fluorescence intensity. Most recently, smFRET and ensemble FRET based on fluorescence lifetime imaging (FLIM-FRET) were used to determine the three-dimensional architecture of high-affinity and low-affinity EGFR–EGF complexes in cells (Webb et al. 2008). By measuring the inter-EGF distances within discrete EGF pairs and the vertical distance from EGF to the plasma membrane, structural and orientation differences in the high- and low-affinity EGFR complexes have been revealed. These findings could explain how EGFR oligomers achieve multiple levels of signaling in normal and diseased cells. smFRET has also been used to detect the binding of BodipyTR-GTP to a G protein Ras-YFP in living cells (Murakoshi et al. 2004), a demonstration that smFRET could be useful for studying the dynamics and activation of G proteins in living cells.
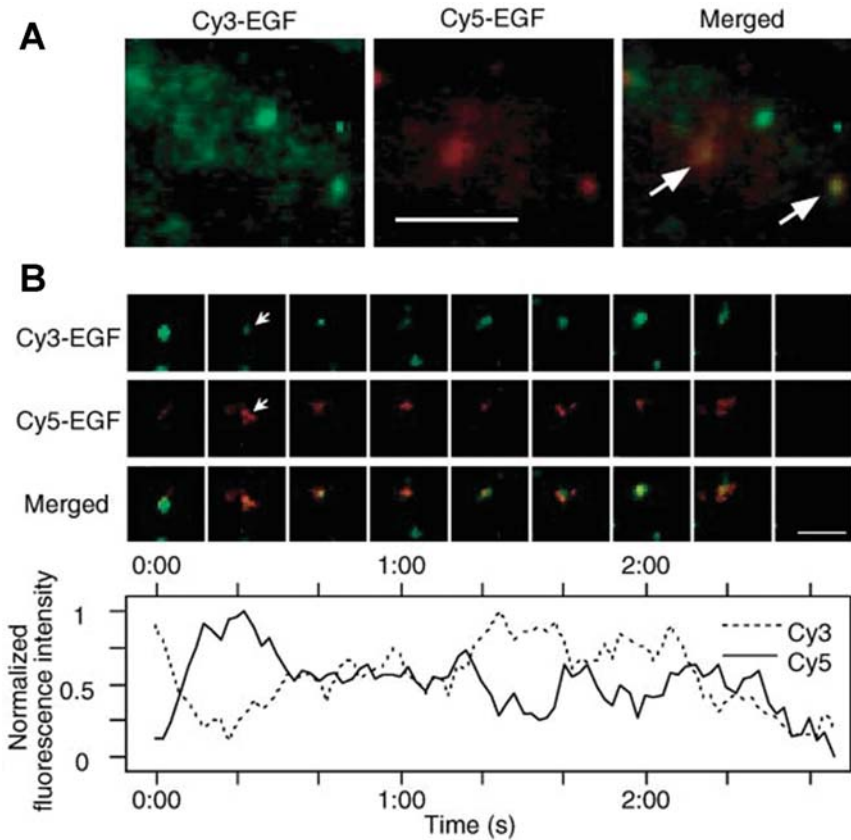
Figure 5.6. Single-molecule fluorescence resonance energy transfer (FRET) between Cy3–epidermal growth factor (EGF) and Cy5–EGF on the surface of living cells. **A.** A mixture of Cy3–EGF and Cy5–EGF was added to A431 cells and imaged with total internal reflection fluorescence microscopy and dual-view optics. Fluorescent spots shown in the Cy5 channel appeared as a result of FRET from Cy3–EGF to Cy5–EGF (*arrows*), indicating interaction between single molecules. **B. Top:** Fluorescence intensity over time of a single spot (*arrow*) was measured in both Cy3 and Cy5 channels. The diffusion of the spot was slow, probably because of slow Brownian motion of EGF receptor (EGFR) bound to the cytoskeleton. **Bottom:** Anticorrelation between Cy3 and Cy5 fluorescence intensities indicated FRET occurring due to the binding of Cy3– and Cy5– EGF on the same EGFR dimer. [Adapted from Sako et al. 2000. Copyright Nature Publishing Group.]

5.7. Applications of Single-Molecule FRET to Biomolecular Systems

Since the first single-molecule FRET experiment measured on doubly labeled DNA molecules immobilized on a glass surface (Ha et al. 1996), smFRET has seen an escalation in applications on biomolecular systems within the last decade. Based on the principle of acting as a nanoscale ruler at 2–10 nm, it can map out molecular distances in three dimensions; monitor conformational changes in real time, and catch molecular motors in action. In this section, we discuss several biomolecular systems to which smFRET has been applied. Due to space limitations, this survey cannot be comprehensive; we discuss mainly applications of single-molecule FRET to the structure, dynamics, and mechanism of nucleic acids, protein–nucleic acid complexes, and selected proteins (molecular motors and protein-folding model proteins). We should mention, however, that smFRET has been used to make contributions to

the understanding of many mechanisms and molecular devices, such as translation (Blanchard et al. 2004a, b), DNA processing (Smiley et al. 2007), homologous recombination (Joo et al. 2006), transcription regulation (Morgan et al. 2005; Schluesche et al. 2007), nucleosome dynamics (Koopmans et al. 2007), membrane fusion (Margittai et al. 2003), and energy transfer in photonic wires (Heilemann et al. 2004).

5.7.1. Applications to Nucleic Acids

Holliday Junctions

One of the first systems extensively studied using single-molecule FRET is the Holliday junction, a four-way DNA junction that constitutes a central intermediate of recombination and DNA replication. The Holliday junction is initially formed after strand exchange between two homologous sequences of two DNA strands; it subsequently undergoes branch migration, a process in which the initial heteroduplex DNA is extended by movement of the junction along DNA. Prior to 2003, it was known that in the absence of Mg^{2+}, the Holliday junction adopts an open structure in which the four helices point to the corners of a square. It was also known that in the presence of Mg^{2+}, the junction folds into a more compact stacked-X structure, in which two neighbouring helices undergo coaxial stacking, leading to two possible stacked structures. However, only one of the stacked structures had been observed using X-ray crystallography; moreover, there was no information about possible transitions between the stacked conformers and no clear understanding of branch migration and its coupling to the transitions between stacked and open conformations of the Holliday junction. A major obstacle for such studies was the inability to synchronise such stochastic conformational changes; single-molecule FRET offered an elegant and direct way to address this limitation and shed light on the thermodynamics and kinetics of the process by observing dynamic transitions between stacked conformers, as well as branch migration.

The first report on the dynamics of Holliday junctions used "immobile" Holliday junctions (junctions with nonhomologous sequences that prevent branch migration) labeled at the ends of two of the helices with a donor and acceptor. Use of confocal microscopy on individual surface-immobilised Holliday junctions led to direct observations of switching between low- and high-FRET states that correspond to the stacked conformers. Analysis of the dwell times at the two states provided the rate constants of the transitions, which were Mg^{2+} concentration dependent, as expected (Hohng et al. 2004; McKinney et al. 2003).

The initial studies on immobile junctions did not report on branch migration. Towards such a goal, McKinney et al. (2005) designed DNA sequences that allow a single–base pair step of branch migration; again, the labeling strategy led to distinct FRET efficiencies for the two stacked conformers. It is intriguing that FRET time traces showed that the junction interconverted between FRET states at two distinct rates (fast and slow), with the rate dependent on the sequence of the central part of the junction; the switch from one rate to the other was interpreted as a branch migration step (since the step changes the central sequence context and therefore the interconversion rate). As previously, the transition rate depended on Mg^{2+} concentration and on the G-C versus A-T content of the central sequence, with the latter having fewer transitions between stacked conformers before branch migration. One surprising finding was that different branch points had more than a 30-fold variation in their lifetimes, which led to the proposal of a highly sequence-dependent energy landscape for spontaneous branch migration. An independent smFRET study on mobile Holliday junctions also studied real-time branch migration over a 5-bp homology region, establishing that branch migration

proceeds in a stepwise pattern and that each step could represent more than a single base pair, with Mg^{2+} modulating the rate of branch migration (Karymov et al. 2005; Karymov et al. 2008a, b). This swift progress in the understanding of the mechanism of branch migration will certainly be followed by extensive analysis of the effect of proteins that recognise and process this important DNA intermediate.

RNA Folding

smFRET was also used extensively in studies of RNA folding. One form of single-stranded RNA folds to form secondary structures with catalytic activity called ribozymes or RNA enzymes. Ribozymes catalyze numerous cellular processes, such as translation and RNA splicing, and are used in biotechnology as therapeutic agents and in functional genomics. Their catalytic activity of performing site-specific cleavage and ligation reactions depends on their folded structures and their interactions. Various biochemical and ensemble techniques have discovered that ribozymes undergo multiple folding pathways and intermediate states to achieve the native structure. However, the characterization of many transient intermediate states was not accessible by ensemble methods that probed only well-populated, accumulative intermediate states. Furthermore, large multidomain ribozymes have complex folding pathways and interactions that make the characterization of each pathway difficult with ensemble methods. smFRET offers additional information that ensemble methods lack by allowing the observation of structural dynamics of transient intermediate states and subpopulations in a heterogeneous system. The first smFRET study on the dynamics of RNA folding used a large multidomain ribozyme (Zhuang et al. 2000) and was discussed in Section 5.3.

Fast conformational kinetics of a two-way junction hairpin ribozyme cleavage pathway was also determined for the first time with smFRET (Zhuang et al. 2002). Based on the use of labels at both ends of the helices, the FRET time traces revealed the folding and unfolding transitions in real time, and their kinetics was determined to have one folding rate of 0.008 sec^{-1} and four other unfolding rates. In addition, the time traces showed a "memory effect" by which similar dwell times were repeated in the folded state and rarely switched between different folded states after unfolding, suggesting four different folded and unfolded states, in which three of them were too few populated and too fast to be detected with ensemble methods. The four-way junction hairpin ribozyme was found instead to have a folding rate that was three to four orders of magnitude faster, with both heterogeneous folding and unfolding kinetics dependent on Mg^{2+} concentration (Tan et al. 2003). FRET time traces provide the history of a given state and allowed the finding of a previously unknown intermediate with a proximal conformation that was obligatory for the folding of the hairpin ribozyme. This intermediate works by folding the loops in close proximity, increasing the probability of interaction and hence speeding up the folding rate. smFRET has demonstrated the robustness of obtaining highly heterogeneous structural and kinetic information of complex RNA folding pathways and rugged energy landscapes, which had been largely an unexplored field.

DNA Nanomachines

DNA nanomachines are examples of DNA nanotechnology (Bath and Turberfield 2007; Rothemund 2006; Seeman 2003; Seeman 2005), a branch of synthetic biology that uses the unique properties of DNA (ease and programmability of DNA hybridization, rigid and

well-understood structure at the 10- to 50-nm scale, facile synthesis and manipulation) to assemble artificial molecular machines that can generate motion and accomplish a specific task as a response to a specific signal. The nanometer measurement scale of FRET is particularly suitable to study the conformational changes of such machinery.

Recently, a novel DNA nanomachine has also been studied with smFRET using microsecond ALEX (Section 5.4). Specifically, Goodman et al. used the specificity of DNA hybridization to prepare self-assembling DNA tetrahedra (Goodman et al. 2004; Goodman et al. 2005) that can reversibly change shape in response to specific signals (Goodman et al. 2008). In the reconfigurable design, one of the edges of the tetrahedron contains a hairpin loop. In the absence of "fuel" the loop remains closed, producing a 10-bp-long edge. When the "fuel" (a single-stranded DNA strand complementary to the hairpin loop) is added, it hybridises to both halves of the hairpin, producing a substantially extended edge (30-bp long). This cycle is reversible, as shown using polyacrylamidegel electrophoresis (PAGE) and ensemble-FRET measurements; the addition of an "antifuel" hairpin complementary to the fuel strand binds and displaces the fuel from the tetrahedra and returns them to the closed state. This cycle can be repeated several times. The FRET measurements were carried out by labeling each end of the hairpin edges with donor and acceptor fluorophores so the closed state would give high FRET and the open state would give low FRET. However, this did not exclude the presence of either static heterogeneity, where the tetrahedra could occupy a range of static partially open states; or dynamic heterogeneity, where the tetrahedra could undergo transient opening. To address this issue, μsALEX was used to measure FRET for the initial conversion to closed and then open tetrahedra. Each state showed a single homogeneous population at expected FRET values, showing that dynamic interconversion was not present on any significant scale.

Müller et al. (2006) used nsALEX/PIE to characterise DNA tweezers (Section 5.4), one of the first DNA machines (Yurke et al. 2000). The principle of DNA tweezers is as follows: Initially the tweezers are in the open, low-FRET state; upon addition of a closing stand ("fuel") that hybridises with the tweezers, the tweezers convert to the closed, high-FRET state. The addition of fuel may produce several DNA nanostructures other than the desired DNA tweezers; such nanostructures will have different FRET efficiencies and stoichiometries difficult to study using ensemble methods because their FRET efficiencies are expected to average out at the ensemble level. However, it was elegantly shown in a single diffusion-based nsALEX/PIE measurement that whereas open tweezers exist in a single conformation, the addition of fuel generated three conformations corresponding to various states of "closed" tweezers. These closed states were tentatively assigned to some of the states seen in the FRET histogram generated by nsALEX/PIE.

These experiments illustrate well how DNA nanotechnology and smFRET methods are natural partners because both are essentially concerned with the properties of single molecules, smFRET can be used to directly report on the structure and function of DNA nanostructures, and this information can then be used to inform the development and design of new nanostructures.

### 5.7.2. Applications to Nucleic Acid Machines

DNA and RNA Helicases

smFRET methods have proven to be a powerful tool for probing the structure and mechanism of helicases in ways not possible with ensemble methods. Helicases are motor

proteins that translocate and unwind double-stranded nucleic acids into their complementary single strands using energy derived from adenosine triphosphate (ATP) or nucleotide hydrolysis. These enzymes are crucial for many cellular processes, such as DNA replication, transcription, repair, and recombination. Whereas the knowledge of helicase mechanistic properties has generally been determined by pre–steady-state kinetic ensemble studies of single turnovers, they only provide overall kinetic information of the unwinding and translocation of DNA, two core mechanisms of the helicase. smFRET can provide high base pair resolution (≤10 bp), resolving the problem of low helicase processivity *in vitro*, and can probe detailed mechanistic processes not detectable by ensemble methods, such as pausing, rewinding, and repetitive shuttling.

The earliest smFRET work on helicase was the investigation of unwinding of double-stranded DNA by *E. coli* Rep helicase (Ha et al. 2002). Based on the use of a donor and acceptor–labeled DNA duplex or biotinylated-Rep immobilized on a surface and imaged using TIRF microscopy, FRET fluctuations showed the translocation of Rep monomer along single-stranded DNA (ssDNA) using ATP hydrolysis, stopping at the junction of ssDNA and dsDNA. At increasing Rep concentrations, DNA unwinding was initiated only with the binding of additional Rep to form a functional oligomer, which was indicative of the rate-limiting step. This result led to the explanation of limited unwinding processivity *in vitro*, in which frequent stalling of the Rep helicase was observed from a partially dissociated Rep oligomer. The stalled state could then proceed in two ways: rewinding of dsDNA upon complete dissociation of Rep or reinitiation of unwinding upon formation of functional Rep oligomer. This revealed new mechanistic information about helicase and raised the questions about the connection of the reactions to the structure or conformations at each reaction state. Crystal structures of Rep helicase showed two different conformations, open and closed, implying the structural flexibility of the helicase. The binding orientation of Rep to DNA was determined, using smFRET, and from powerful triangulation methods of eight different donor-labeling sites and an acceptor labeled at the ssDNA/dsDNA junction, the Rep monomer was found mainly to be in the closed conformation when bound to the DNA junction, a conformation representing an inactive state of the Rep helicase (Rasnik et al. 2004). Single-molecule FRET was also used to identify an unexpected translocation mode for Rep helicase: its repetitive shuttling motion on DNA (Myong et al. 2005). The FRET increased as a donor-labeled Rep at the 3′ end of ssDNA translocated towards the acceptor at the 5′ end (Figure 5.7). As the Rep monomer stopped translocation when it encountered the ssDNA/dsDNA junction, it snapped back to its initial position and repeated this shuttling, producing a saw-toothed pattern in the FRET time trace. The functionality of the repetitive shuttling was proposed to keep the ssDNA clear of unwanted proteins such as toxic recombination intermediates.

Helicases can be characterized by their step sizes upon translocation or unwinding of DNA or RNA. Single-molecule FRET was used to study the RNA-unwinding mechanism by nonstructural protein 3 (NS3; an essential helicase for replication of hepatitis C virus) and showed that NS3 unwinds DNA (used instead of RNA due to ease of synthesis) at discrete steps of 3 bp. In the dwell-time analysis of each FRET state, the unwinding proceeded in a proposed spring-loaded mechanism where domains 1 and 2 of NS3 translocated three hidden steps consisting of one ATP hydrolysis each while domain 3 remained fixed. This accumulated tension on the NS3–DNA complex, which was released by unwinding abruptly in a 3-bp step (Myong et al. 2007).
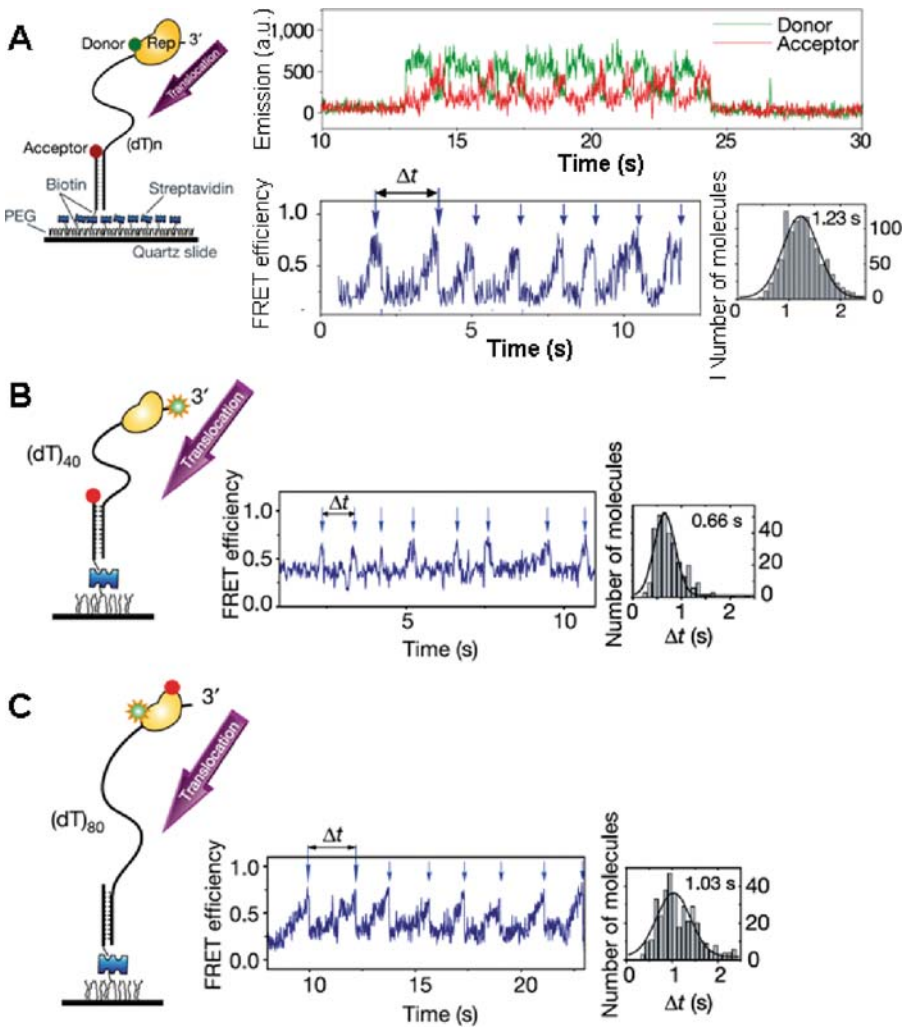
Figure 5.7. Repetitive shuttling of Rep Helicase on single-stranded DNA (ssDNA). Rep helicase was donor-labeled and applied to acceptor-labeled ss/double-stranded (ds) DNA molecules immobilized on a PEGylated surface. Fluorescence intensity time traces displayed anticorrelation between green and red intensity and the fluorescence resonance energy transfer (FRET) trace, pointing to Rep translocation towards the acceptor (gradual increase in FRET), followed by an unexpected snapback (sharp drop in FRET) as it hits a blockade at the junction of ss/dsDNA. **B.** Mechanism of repetitive shuttling. An unlabeled Rep was added to DNA labeled at both ends. The FRET trace showed regular spikes of high FRET, demonstrating the forming of a temporary ssDNA loop as Rep is simultaneously bound to the 3′ end and the ss/dsDNA junction. **C.** Conformation of Rep. Rep helicase was labeled with both a donor and an acceptor. The FRET trace showed a gradual increase as Rep gradually adopts an open conformation as it translocates towards the junction, then closes abruptly as it snaps back. PEG, poly(ethylene glycol). [Adapted from Myong et al. 2005. Copyright 2005 Nature Publishing Group.]

DNA Polymerase

Since the completion of the human genome sequence using the Sanger sequencing method and the subsequent launch of many other genome projects, there has been a race to develop faster, cheaper, and more sensitive sequencing methods. The specificity and reproducibility of DNA polymerase (DNAP) enzyme can be exploited to image sequence information on a DNA template during the synthesis of the complementary strand, as shown by several recent examples (Guo et al. 2008; Harris et al. 2008). The first report that demonstrated DNA sequencing by smFRET performed cyclic synthesis by DNAP using TIRF microscopy (Braslavsky et al. 2003). The sequencing assay involved a surface-immobilised DNA template with an annealed donor-labeled primer and the flowing of DNAP and labeled nucleotide triphosphates while the DNA template positions monitored for FRET signal. The reagent exchange for smFRET sequencing proceeded as follows: The position of the donor-labeled DNA primer was recorded and the donor was bleached before the first round of incorporation. This round consisted of donor-labeled nucleotides deoxyuridine triphosphate (dUTP)–Cy3 or deoxycytidine triphosphate (dCTP)–Cy3 with DNAP, which was flowed in and checked for donor signal. Unlabeled deoxyadenosine triphosphate (dATP), deoxyguanosine triphosphate (dGTP), and DNAP were then flowed in to extend the primer until the next A or G. If there was no donor signal detected for the first incorporation, this process was repeated. Otherwise, the second round of incorporation used acceptor-labeled nucleotides dUTP–Cy5 and dCTPxCy5 and checked for FRET signal, followed by bleaching the acceptor before flowing unlabeled dATP, dGTP, and RNAP. Green and red lasers were alternated to excite the donor, check for FRET, and bleach the acceptor. This whole cycle was repeated several times. This method of sequencing DNA allowed the determination of sequence fingerprints up to 5 bp in length with 97% confidence level. However, this FRET assay was limited by the dynamic range of FRET at 5 nm, thus restricting the read length equivalence to ~15 bases. Instead, labeling DNAP with a donor and monitoring the FRET signal as it incorporates acceptor-labeled nucleotides may overcome this constraint. Nevertheless, Braslavsky et al.'s pioneering work on using DNAP and FRET between labeled nucleotides has been instrumental for the development of subsequent generations for DNA sequencing.

RNA Polymerase

RNAP is the multifunctional machine at the heart of transcription, one of the most important biological processes in gene expression and regulation. RNAP works by recognizing specific sites on the DNA, unwinding the DNA helix around the start site, and transcribing the DNA by synthesizing a complementary RNA strand. There have been numerous studies on the structure and function of RNAP and the mechanism of transcription at initiation, elongation, and termination. Recent papers have reviewed extensively the studies of RNAP transcription with single-molecule methods (Bai et al. 2006; Herbert et al. 2008).

One of the first questions addressed using single-molecule FRET involved the fate of the bacterial transcription initiation protein σ^{70}. Early observations of σ^{70} absence in RNAP–DNA elongation complexes led to proposals that σ^{70} release is required for the transition from transcription initiation to elongation and that the molecular machinery in transcription is essentially different between initiation and elongation. Kapanidis et al. (2005) used single-molecule FRET combined with ALEX to measure the extent of σ^{70} retention at various points along elongation. The ALEX-based σ^{70} release assay was based on observations of changes

in intermolecular distances and binding stoichiometries upon escape to elongation. The assay uses analytical sorting to distinguish between σ^{70} retention and σ^{70} release in elongation: For a leading-edge FRET assay (which uses a donor introduced at the leading edge of RNAP and an acceptor at the downstream end of DNA), forward translocation and formation of a σ^{70}-containing elongation complex converts a donor–acceptor species with low FRET to a donor–acceptor species with high FRET; on the other hand, formation of $\sigma70$-free elongation complex with release of σ^{70} converts a donor–acceptor species with low FRET to donor-only and acceptor-only species, which can be identified using the stoichiometry dimension of ALEX histograms. The results show clearly that σ^{70} release is not obligatory but stochastic, with 70%–90% of early elongation complexes and 50%–60% of mature elongation complexes retaining σ^{70}. The long half-life of σ^{70} in mature elongation complexes suggested that some complexes might retain σ^{70} throughout elongation, allowing multiple additional levels of gene regulation with σ^{70}.

The mechanism of initial transcription in which RNAP translocates relative to DNA had also been controversial. Based on ensemble biochemical results, there were three proposed models that attempted to describe the physical mechanism of the process: first, the model of transient excursions, which invoked transient cycles of forward/reverse translocation of RNAP; second, the model of RNAP inchworming, which invoked a flexible element in RNAP that translocates downstream during abortive RNA synthesis and retracts upon release of the abortive RNA; and third, the model of DNA scrunching, which invoked a flexible element in DNA that was pulled in by a fixed RNAP during translocation and extruded upon release of the abortive RNA (Figure 5.8A). The three models were tested by monitoring the open complex and initial transcribing complexes labeled at different positions on RNAP and on promoter DNA (Kapanidis et al. 2006). Based on the changes in FRET efficiencies, it was shown that the only distances changing during abortive transcription were distances between DNA downstream of the transcription bubble and the RNAP leading edge, as well as between
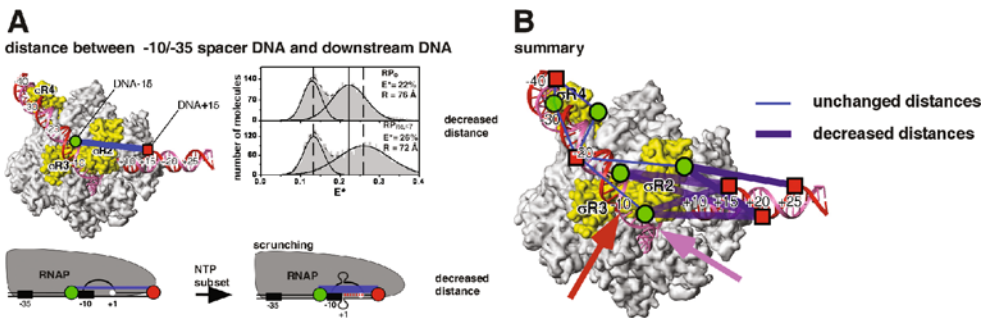
Figure 5.8. Initial transcription involves DNA scrunching. **A.** Experiment documenting the contraction of DNA between positions –15 (Cy3b) and +15 (Alexa647). Subpanels show E^* histograms of open complex (RP$_\text{o}$) and initial transcribing complexes with up to 7-nt RNA (RP$_{\text{itc}, \leq 7}$). The histograms comprise free DNA (lower-E^* species) and the RNA polymerase (RNAP)–DNA complexes (higher-E^* species attributable to RNAP-induced DNA bending). Free DNA is present in all experiments. The increase in the fluorescence resonance energy transfer (FRET) efficiency in RP$_{\text{itc}, \leq 7}$ (compared to RP$_\text{o}$) point to DNA compaction during abortive initiation, consistent with the predictions of the DNA-scrunching model (see text for details). **B.** Structural model of RP$_\text{o}$ showing all donor–acceptor distances monitored. Thin blue lines represent distances that remain unchanged on transition from RP$_\text{o}$ to RP$_{\text{itc}, \leq 7}$. Thick blue lines represent distances that decrease on transition from RP$_\text{o}$ to RP$_{\text{itc}, \leq 7}$. Red and pink arrows show the proposed positions at which scrunched template (–9 to –10) and nontemplate strand DNA (–5 to −6), respectively, emerge from RNAP.

DNA downstream of the transcription bubble and DNA upstream of the transcription bubble (Figure 5.8B). This validated the scrunching mechanism and supported a model in which the stress accumulated from the DNA unwinding and compaction drives the breaking of bonds between RNAP and DNA into promoter escape and elongation. Conformational heterogeneity of RNAP during elongation (Coban et al. 2006) and the scrunching and rotation of T7 RNAP during initiation has also been observed with smFRET (Sharma et al. 2008).

Reverse Transcriptase

Reverse transcriptase (RT), in particular the human immunodeficiency virus type 1 (HIV-1) RT, is a nucleic acid polymerase that uses RNA as a template to synthesize double-stranded DNA for integration into the host genome. RT is a heterodimer consisting of a p51 and p66 subunit, with the latter containing RNA- and DNA-dependent DNA polymerase activities and an RNase H domain. Crystallographic studies of the RT–nucleic acid complexes showed a single primer/template binding mode, but recent ensemble kinetic studies suggested a heterogeneous mixture of several binding modes. To determine the existence of several species and obtain functional and structural information of each, the group of Claus Seidel developed a multiparameter fluorescence detection technique (MFD) that measures FRET based on the reduction of donor lifetimes (Rothwell et al. 2003). The group investigated donor-labeled RT at the p66 domain and acceptor-labeled primer to reveal three distinct states of RT–nucleic acid complexes. One of the states, not seen before by X-ray crystallography, did not incorporate nucleotides and was structurally different from the other two. The other two states were similar to the crystal structure but differed only by 5Å in the nucleic acid position from each other. The two states undergo conformational changes upon binding a nucleotide, allowing the researchers to assign the structures as productive stages in DNA polymerization.

The mechanism of RT that coordinates the DNA polymerase and RNase H activities is unknown. Although RNase H cleavage analysis has shown different interaction modes with substrates, crystal structures have only shown one enzyme-binding orientation. To address this question and study RT binding conformations, an smFRET assay with msALEX was used (Abbondanzieri et al. 2008). Surface-immobilised DNA or RNA substrate was acceptor-labeled at the 5′ or 3′ end and immersed in a solution containing free RT molecules, donor-labeled either at the RNase H domain or at the fingers subdomain (at the DNA polymerase domain) on the p66 subunit. The distinct FRET efficiencies showed that RT binds DNA and RNA primers in opposite directions, hence defining its enzymatic activity. For the binding of RT to duplexes containing polypurine RNA primers for plus-strand DNA synthesis, RT was found to dynamically switch between binding orientations. Cognate nucleotides and nonnucleoside RT inhibitors, a class of anti-HIV drugs, were found to have opposing effects on switching rates. The dynamic conformational changes of RT binding to substrates allowed the enzyme to explore multiple binding orientations, thereby regulating enzymatic kinetics and replication efficacy. This provided new insights into the dynamic structure and function of RT that had not been shown before with ensemble methods or crystal structures and could help in the development of pharmacological agents.

5.7.3. Applications to Molecular Motors

Molecular motors are proteins that use the energy from nucleotide hydrolysis to transport cargoes in cells and exert mechanical tension. Motor proteins have been extensively studied by single-molecule methods (especially optical traps and single-molecule fluorescence)

that revealed the stepping characteristics of each motor, the energy requirements, the determinants, and conformational changes occurring during each stepping cycle. Single-molecule FRET has also contributed to the improved understanding of two of these motor proteins: linear motor kinesin and rotary machine F_0F_1-ATP synthase. In both cases, FRET pairs were incorporated in the molecular motor, either in different subunits or within a single subunit, and conformational changes were observed during the motor's function.

ATP Synthase

F_0F_1-ATP synthase is a multi-subunit molecular machine that uses the proton-motive force (a transmembrane gradient of proton concentration) to generate ATP from adenosine diphosphate (ADP) and phosphate in the membranes of mitochondria, chloroplasts, and bacteria. The machine can also work in reverse, consuming ATP molecules to translocate protons across membranes, and it consists of two coupled components: a membrane-bound hydrophobic part (F_0) responsible for proton translocation and a hydrophilic part (F_1) responsible for ATP hydrolysis and synthesis (Figure 5.9A). A salient feature of the motor is the presence of a multisubunit rotor (subunit composition of $\gamma\epsilon c_{10\text{-}12}$) that rotates 120° per step (with one step corresponding to the synthesis or consumption of a single ATP) with regards to a stator assembly (subunit composition of $\alpha_3\beta_3\delta ab_2$) and the rest of the protein, with each β subunit containing an ATP-binding site. Extensive biochemical, structural, and single-molecule studies have made this rotary motor one of the best-studied proteins in bioscience (Abrahams et al. 1994; Boyer et al. 2000) and inspired some of the most elegant and ground-breaking single-molecule experiments (Noji et al. 1997). Despite this impressive body of work, a full understanding of the mechanism of coupling of the two main functions of the protein is first beginning to emerge.

The first single-molecule FRET on the motor (Borsch et al. 2002) examined the intact F_0F_1 proteins reconstituted in liposomes, a system more complex that the F_1 part used for initial single-molecule fluorescence studies (Noji et al. 1997). Single-molecule FRET is well suited for studying the rotary motion because it is stochastic and cyclic and, as such, it cannot be synchronised and dissected at the ensemble level. The rotation of the γ subunit versus the rest of the protein was observed by placing a donor on the b subunit of F_0F_1 and an acceptor on the γ subunit (Figure 5.9A). Upon rotation of the γ subunit, a stepwise change in FRET states was expected due to the stepwise changes among the three different donor–acceptor distances corresponding to the three main conformations of the γ subunit against the rest of the protein (similar to the conformations in Figure 5.9B). The first experiments used a confocal setup with ~1-ms temporal resolution to observe diffusing liposomes with single F_0F_1 molecules. Analysis of fluorescence intensity and FRET time traces led to observation of the predicted switching among three FRET states during the diffusion of one membrane-bound F_0F_1 molecule through an expanded confocal volume (Figure 5.9C). Of importance, the rate of FRET transitions due to presumed rotation matched the rate of ~30 sec^{-1} obtained from enzymatic assays performed for this protein preparation. In further studies of F_0F_1 using a revised labeling scheme (Diez et al. 2004), an improved temporal resolution, and additional FRET information (arising from donor-lifetime analysis), it was shown that the γ subunit rotates in a stepwise fashion (as opposed to continuously) during ATP synthesis and in a direction opposite to the rotation observed during ATP hydrolysis (Figure 5.9D, E). Similar results were obtained when a fluorophore was introduced in the ϵ subunit, which also forms part of the rotor assembly (Zimmermann et al. 2006).
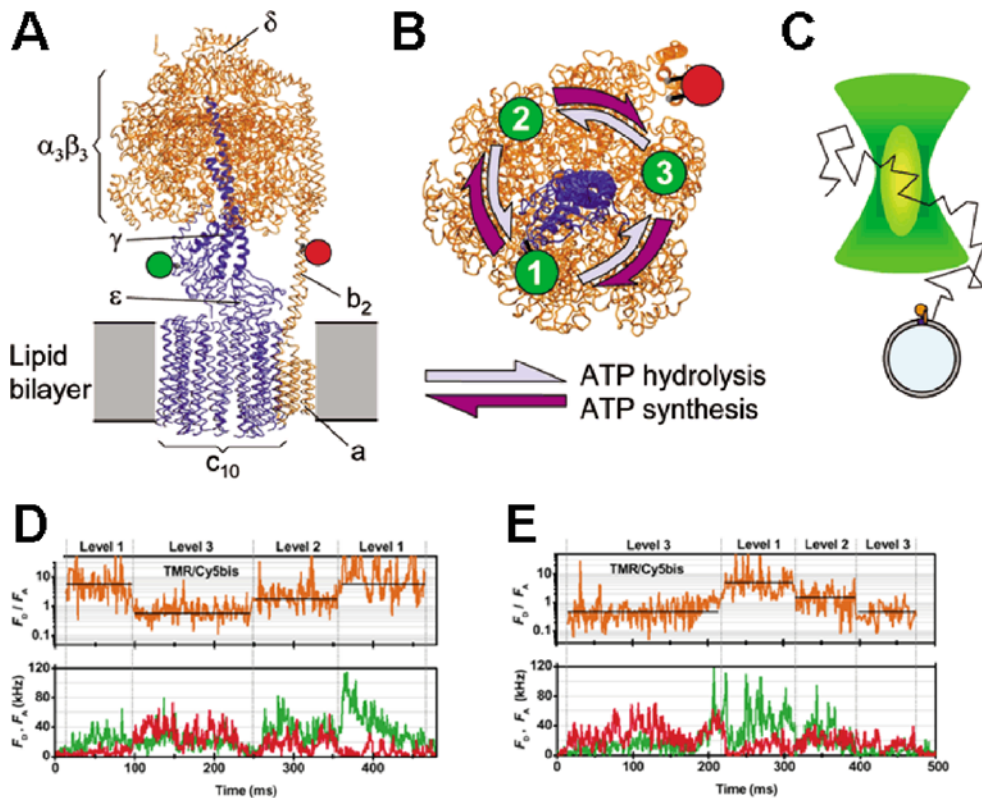
Figure 5.9. Single-molecule fluorescence resonance energy transfer (FRET) studies of adenosine triphosphate (ATP) hydrolysis and synthesis by ATP synthase. **A.** Side view of a model of bacterial F_1F_0-ATP synthase integrated in a lipid bilayer along with FRET probes. The rotor assembly is in blue, and the stator assembly is in orange. The donor (*green circle*) is attached to the γ subunit, and the acceptor (*red circle*) is attached to the b_2 subunit. **B.** Top view of a cross section of the model shown in panel A. Rotation of the stator generates three distinct FRET states in a cyclic fashion. ATP hydrolysis causes counterclockwise rotation, whereas ATP synthesis leads to clockwise rotation. **C.** Experimental format. Diffusing labeled ATP-synthase molecules in liposomes cross a confocal volume and generate long fluorescence bursts (see panels D and E). **D.** Photon bursts from ATP-synthase molecules during ATP hydrolysis show cycling among three FRET states (represented by three levels of the ratio F_D/F_A, which depends on FRET efficiency). **E.** Photon bursts from ATP-synthase molecules during ATP synthesis show cycling along three FRET states in a direction opposite to the one for ATP hydrolysis. [Adapted from Diez et al. (2004). Copyright 2004 Nature Publishing Group]
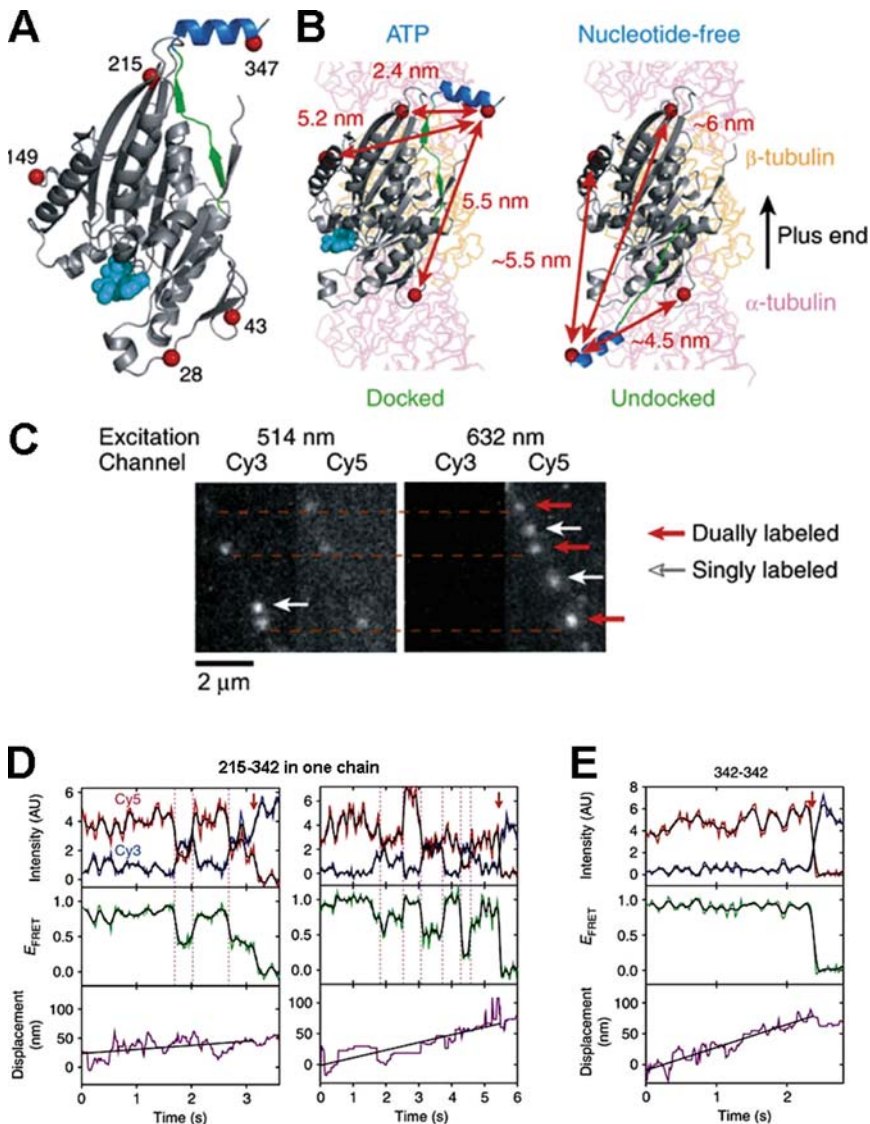
Kinesin

Kinesin, one of the smallest molecular motors in cells, is a dimeric protein that uses the energy of ATP to move cargoes towards the plus end of microtubules (Vale 2003). Kinesin has been the focus of extensive biochemical, structural, and biophysical studies, which have showed that kinesin moves in 8-nm steps by a hand-over-hand processive motion (Yildiz et al. 2004). The group of Ron Vale was the first to use FRET methods to look at conformational changes while kinesin reconfigures itself during its mechanochemical cycle, either using static measurements (e.g., Rice et al. 1999) or by probing kinesins in action on microtubules.

The first application of smFRET to the study of kinesin (Tomishige et al. 2006) examined conformations of the neck-linker region of kinesin, a 12–amino acid region crucial for the coordination of biochemical activities and conformational changes within each kinesin step (Figure 5.10A). From prior work, it was known that the neck region adopts a "docked" (forward-extending) state in the presence of ATP and an undocked state (backward-extending) in the presence of ADP or in the nucleotide-free state (Figure 5.10B). These observations led to a model in which ATP conversion to ADP in the leading head of the kinesin leads to docking of the neck-linker region and to a ∼16-nm movement of the trailing head towards the direction of motion. Previous attempts to test this model were complicated by ensemble averaging of conformations (e.g., both linkers were labeled in a kinesin homodimer) and by operating at high ATP concentrations, where transitions between linker conformers are too fast to be resolved directly. To identify the different conformations of the neck linker and to see dynamic changes in neck-linker conformations as kinesins move on axonemes, the group prepared kinesins in which only a single neck linker was labeled with a FRET pair. To achieve this challenging task, the group used a tour-de-force of site-directed mutagenesis, labeling, and functional assays to identify six labeling positions with kinesin that did not affect function.

Using a TIRF microscope and alternating-laser excitation, it was possible to identify kinesins with a donor and an acceptor and generate FRET histograms for several interprobe positions and nucleotide states. This experiment was a static one, providing equilibrium distributions of FRET efficiencies; the FRET analysis confirmed the expected docked conformation for the ATP-bound state (using a nonhydrolyzable analog of ATP) and the undocked conformation for the nucleotide-free state. The group went on to study transitions between conformations in real time by tracking doubly labeled kinesins as they moved on microtubules (Figure 5.10C); this impressive experiment combined tracking of a large-scale, "global" probing of the unidirectional movement of kinesin along with "local" probing of the intrasubunit conformational changes occurring during each step. Indeed, at low ATP concentrations (∼1 μM), the group succeeded in observing transitions between dwells in high- and low-FRET states that represent docked and undocked states, respectively, for the FRET pair used (Figure 5.10D).

This first application of smFRET to kinesin dynamics was followed by a study that addressed the question of the prevailing conformation of kinesin while it waits for the second ATP molecule to bind between steps (Mori et al. 2007). The group this time used two FRET pairs that examined intersubunit distances within kinesin heterodimers. An initial calibration using static distributions of kinesins showed that in the presence of an ATP analog, a two-head-bound state predominates, whereas in the presence of low ADP, states in which the heads come closer to each other (before dissociation) are populated; these states were interpreted as one-head-bound states, which was confirmed using a heterodimeric kinesin able to bind only through a single head.

The most interesting conclusions of this work came from studies on FRET-labeled kinesin molecules moving on microtubules. At saturating ATP conditions, kinesins occupy FRET states consistent with a two-head-bound state, pointing to the fact that the time spent in the one-head-bound state is very small. In contrast, at limiting ATP concentrations, the predominant FRET state is consistent with an one-head-bound state interdispersed with transitions to lower- and higher-FRET states, which are interpreted as transient two-head-bound states (mostly towards a forward direction). This detailed experimental treatment of such a complex system allowed formulation of an updated model for kinesin translocation at different levels of ATP and explained some inconsistencies existing in the field.

Figure 5.10. Single-molecule fluorescence resonance energy transfer (smFRET) measurements of kinesin dynamics. **A.** Model of kinesin showing labeling sites (*red spheres*) used in Tomishige et al. (2006). The neck linker (*green*) is in the docked conformation; adenosine diphosphate (ADP) is shown as a cyan space-fill. **B.** Intraprotein distances between labeling sites for the adenosine triphosphate (ATP)–bound, docked state of kinesin and for the nucleotide-free, undocked state of kinesin. **C.** Experimental format. Sequential excitation by 514- and 632-nm light and wide-field imaging identifies singly- and doubly- labeled kinesins on surface-immobilised microtubules. **D.** FRET fluctuations due to conformational changes in the neck linker during the motion of kinesins along microtubules at low ATP concentration. The donor and intensity time traces **(top)** are used to calculate FRET efficiencies **(middle)** during the motion of doubly labeled kinesins; kinesin motion is tracked by localising the fluorophores **(bottom)**. Abrupt and large changes in FRET are due to conformational changes in the neck linker. **E.** Negative control (heterodimeric kinesin 342-342) shows no significant conformational changes under conditions identical to ones used in panel D. [Adapted from Tomishige et al. 2006. Copyright 2006 Nature Publishing Group.]

5.7.4. Applications to Protein Folding and Dynamics

The multistep nature of protein folding and dynamics means that bulk measurements can only provide ensemble-averaged information on the process, whereas theory and simulations consider folding on the single-molecule or subpopulation level. By contrast, single-molecule methods allow direct observation of individual proteins under various experimental conditions for extended periods. As a result, smFRET has found numerous applications to the study of protein folding and dynamics smFRET approaches have been discussed in recent excellent reviews (Michalet et al. 2006; Schuler and Eaton 2008; Zhuang and Rief 2003). The general approach used for investigations of folding with smFRET has been to study labeled proteins in varying concentrations of denaturant, using the ability of smFRET to monitor individual molecular subpopulations to resolve the folded and unfolded states and thus obtain novel information on folding mechanisms and pathways.

The first smFRET study of protein folding by Deniz et al. (2000), used diffusion methods to directly confirm a two-state model of folding for the chymotrypsin inhibitor and extract free energy landscapes for the protein under varying concentrations of denaturant. This work was extended by a similar study (Schuler et al. 2002) on a doubly-labeled cold-shock protein (Csp). After careful comparison with a series of rigid standards, Schuler et al. recovered a limit in the reconfiguration time for the polypeptide chain in the unfolded state, an important parameter not available from ensemble measurements. The studies on Csp were further extended by measurements of the kinetics of folding in a microfabricated laminar-flow mixing device (Lipman et al. 2003).

Parallel studies have applied surface immobilisation approaches with great success, observing folding kinetics for extended periods of time. After early observations of protein folding on silanized surfaces that may have influenced the folding landscape to a certain degree (Talaga et al. 2000), Rhoades et al. (2003) used the interesting method of encapsulation of labeled proteins in surface-tethered 100-nm lipid vesicles to avoid any surface interactions and found evidence for multiple folding pathways for the folding of adenylate kinase. Kuzmenkina et al. (2005) used surface immobilisation to investigate the dynamics of ribonuclease HI under varying concentrations of denaturant, successfully obtaining a partial free energy landscape for the protein and providing strong evidence that the protein retains significant residual nonrandom structure even in the unfolded state. Recent work has also studied the mechanisms of chaperonin-mediated protein folding (Sharma et al. 2008) and provided strong evidence for the proposal that protein confinement by GroEL/GroES stretches apart strongly hydrophobic regions of a polypeptide and thus opens up folding pathways inaccessible to spontaneous hydrophobic collapse.

smFRET has also been used to study the fundamental mechanisms of enzymatic catalysis. Henzler-Wildman et al. (et al. 2007) studied the enzymatic reaction trajectory of adenylate kinase (Adk) using a number of methods, including smFRET both in solution and on the surface. Adk was fluorescently labeled and monitored in the ligand-bound and ligand-free states (Figure 5.11A). Solution smFRET measurements showed that a state similar to the closed state was significantly populated even in the absence of ligand (Figure 5.11A). Surface-immobilised measurements (Figure 5.11B–D) supported this finding and, by analysing the intensity correlation function (Figure 5.11G), provided estimated interconversion rates between the ligand free open and closed states that agreed well with nuclear magnetic resonance (NMR) data, which had indicated the presence of interconverting states but was unable to determine the amplitude of any dynamics. By combining NMR, molecular dynamics, and smFRET measurements, this research provided strong evidence that
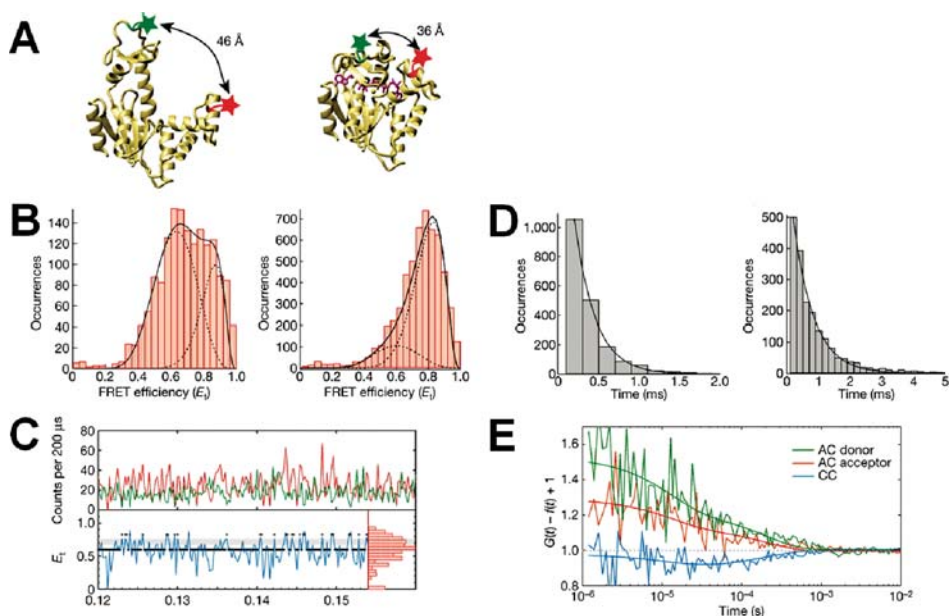
Figure 5.11. Using single-molecule fluorescence resonance energy transfer (smFRET) to study the enzymatic reaction trajectory of adenylate kinase (Adk). **A.** Adk was fluorescently labeled and monitored in the ligand-free and ligand-bound state. **B.** Histograms of FRET efficiencies of ligand-free **(left)** and ligand-bound Adk **(right)** measured from single-molecule diffusion experiments. The dashed lines represent Gaussian fits of the corresponding distance histograms back-transformed into FRET efficiency E_t, and the solid line is the sum of those distributions. The ligand-free state shows a state similar to the closed state, significantly populated even in the absence of ligand. **C.** Section of a single-molecule fluorescence time trace of ligand-free Adk tethered on a glass surface. Donor (*green*) and acceptor (*red*) intensities are shown together with the corresponding E_t (*blue*), including the E_t histogram over 25 time traces (*red, right*). Lifetimes of the open and closed state (*black lines*) were determined using a transition zone for E_t values where the Gaussian distributions of the open and closed states overlap (*grey*). **D.** Resulting lifetimes of 25 time traces were averaged, fitted exponentially, and corrected for missed events and triplet-state dynamics to yield $k_{open} = 6,500 \pm 500 \text{ sec}^{-1}$ **(left)** and $k_{closed} = 2,000 \pm 200 \text{ sec}^{-1}$ **(right)**, respectively. **E.** The intensity correlation function $G(t)$ for autocorrelation (AC) and cross-correlation (CC) analysis for six immobilized ligand-free Adk molecules was calculated to obtain the overall opening/closing rate. Anticorrelation of the CC function is observed in the $10^{-4}-10^{-3}$ sec timescale with a fitted overall opening/closing rate of $7,000 \pm 2,000 \text{ sec}^{-1}$. [Adapted from Henzler-Wildman (2007). Copyright 2007 Nature Publishing Group.]

adenylate kinase samples states resembling the catalytically active closed conformation even in the absence of ligand binding, with implications for the theory of dynamics of enzymatic catalysis.

5.8. Conclusion and Future Prospects

The applications discussed show clearly that single-molecule FRET has affected several fields in basic and applied biosciences. However, there is also room for improvement that will help the implementation and interpretation of smFRET measurements. Moreover, as the research community becomes more familiar with the method, more challenging applications are being considered, raising the bar for single-molecule FRET. Some of the active

areas under development were outlined in Section 5.6. Moreover, advances in site-specific labeling technologies (Deniz et al. 2008; Kapanidis et al. 2001) will expand the number of FRET pairs and overcome distance constraints that can be incorporated into proteins to study protein structure, protein dynamics, and conformational changes. New buffer components that delay photobleaching (e.g., Vogelsang et al. 2008) and control fluorophore photophysics (e.g., Rasnik et al. 2006), as well as the development of reliable quantum-dot biolabels (Bruchez et al. 1998; Michalet et al. 2005) will lead to extended and uninterrupted recordings in a variety of *in vitro* experiments. Ways to achieve this in living cells will enable exciting smFRET experiments in a natural context. Finally, the appeal of the method for observing molecular interactions will increase if the working concentration can be extended to study fluorescent species in concentrations greater than nanomolar range. This may be achieved by combining smFRET with methods that confine the laser excitation volume (Foquet et al. 2004; Levene et al. 2003; Vogelsang et al. 2007) or by using nonfluorescent analytes. Advances in all these aspects, along with improvements in detector technologies and FRET data-analysis algorithms (McKinney et al. 2006), will keep single-molecule FRET in the limelight for years to come.

References

Abbondanzieri EA, Bokinsky G, Rausch JW, Zhang JX, Le Grice SFJ, Zhuang XW. 2008. Dynamic binding orientations direct activity of HIV reverse transcriptase. Nature 453(7192):184–9.

Abrahams JP, Leslie AG, Lutter R, Walker JE. 1994. Structure at 2.8 A resolution of F1-ATPase from bovine heart mitochondria. Nature 370(6491):621–8.

Ambrose WP, Goodwin PM, Martin JC, Keller RA. 1994. Alterations of single-molecule fluorescence lifetimes in near-field optical microscopy. Science 265(5170):364–7.

Andrecka J, Lewis R, Bruckner F, Lehmann E, Cramer P, Michaelis J. 2008. Single-molecule tracking of mRNA exiting from RNA polymerase II. Proc Natl Acad Sci USA 105(1):135–40.

Axelrod D. 2001. Total internal reflection fluorescence microscopy in cell biology. Traffic 2(11):764–74.

Bai L, Santangelo TJ, Wang MD. 2006. Single-molecule analysis of RNA polymerase transcription. Annu Rev Biophys Biomol Struct 35:343–60.

Bath J, Turberfield AJ. 2007. DNA nanomachines. Nat Nanotechnol 2(5):275–84.

Betzig E, Chichester RJ. 1993. Single molecules observed by near-field scanning optical microscopy. Science 262(5138):1422–5.

Betzig E, Trautman JK. 1992. Near-field optics: microscopy, spectroscopy, and surface modification beyond the diffraction limit. Science 257(5067):189–95.

Blanchard SC, Gonzalez RL, Kim HD, Chu S, Puglisi JD. 2004a. tRNA selection and kinetic proofreading in translation. Nat Struct Mol Biol 11(10):1008–14.

Blanchard SC, Kim HD, Gonzalez RL Jr, Puglisi JD, Chu S. 2004b. tRNA dynamics on the ribosome during translation. Proc Natl Acad Sci USA 101(35):12893–8.

Borisenko V, Lougheed T, Hesse J, Fureder-Kitzmuller E, Fertig N, Behrends JC, Woolley GA, Schutz GJ. 2003. Simultaneous optical and electrical recording of single gramicidin channels. Biophys J 84(1):612–22.

Borsch M, Diez M, Zimmermann B, Reuter R, Graber P. 2002. Stepwise rotation of the gamma-subunit of EF(0)F(1)-ATP synthase observed by intramolecular single-molecule fluorescence resonance energy transfer. FEBS Lett 527(1–3):147–52.

Boyer LA, Shao X, Ebright RH, Peterson CL. 2000. Roles of the histone H2A-H2B dimers and the (H3-H4)(2) tetramer in nucleosome remodeling by the SWI-SNF complex. J Biol Chem 275(16):11545–52.

Braslavsky I, Hebert B, Kartalov E, Quake SR. 2003. Sequence information can be obtained from single DNA molecules. Proc Natl Acad Sci USA 100(7):3960–4.

Bruchez M, Jr., Moronne M, Gin P, Weiss S, Alivisatos AP. 1998. Semiconductor nanocrystals as fluorescent biological labels. Science 281(5385):2013–6.

Clamme JP, Deniz AA. 2005. Three-color single-molecule fluorescence resonance energy transfer. Chemphyschem 6(1):74–7.

Clegg RM. 1992. Fluorescence resonance energy transfer and nucleic acids. Methods Enzymol 211:353–88.

Clegg RM. 1995. Fluorescence resonance energy transfer. Curr Opin Biotechnol 6(1):103–10.

Clegg RM, Murchie AI, Zechel A, Lilley DM. 1993. Observing the helical geometry of double-stranded DNA in solution by fluorescence resonance energy transfer. Proc Natl Acad Sci USA 90(7):2994–8.

Coban O, Lamb DC, Zaychikov E, Heumann H, Nienhaus GU. 2006. Conformational heterogeneity in RNA polymerase observed by single-pair FRET microscopy. Biophys J 90(12):4605–17.

Dale RE, Eisinger J, Blumberg WE. 1979. The orientational freedom of molecular probes. The orientation factor in intramolecular energy transfer. Biophys J 26(2):161–93.

Deniz AA, Dahan M, Grunwell JR, Ha T, Faulhaber AE, Chemla DS, Weiss S, Schultz PG. 1999. Single-pair fluorescence resonance energy transfer on freely diffusing molecules: observation of Förster distance dependence and subpopulations. Proc Natl Acad Sci USA 96(7):3670–5.

Deniz AA, Laurence TA, Beligere GS, Dahan M, Martin AB, Chemla DS, Dawson PE, Schultz PG, Weiss S. 2000. Single-molecule protein folding: diffusion fluorescence resonance energy transfer studies of the denaturation of chymotrypsin inhibitor 2. Proc Natl Acad Sci USA 97(10):5179–84.

Deniz AA, Mukhopadhyay S, Lemke EA. 2008. Single-molecule biophysics: at the interface of biology, physics and chemistry. J R Soc Interface 5(18):15–45.

Diez M, Zimmermann B, Borsch M, Konig M, Schweinberger E, Steigmiller S, Reuter R, Felekyan S, Kudryavtsev V, Seidel CA, et al. 2004. Proton-powered subunit rotation in single membrane-bound F0F1-ATP synthase. Nat Struct Mol Biol 11(2):135–41.

Edel JB, Eid JS, Meller A. 2007. Accurate single molecule FRET efficiency determination for surface immobilized DNA using maximum likelihood calculated lifetimes. J Phys Chem B 111(11):2986–90.

Foquet M, Korlach J, Zipfel WR, Webb WW, Craighead HG. 2004. Focal volume confinement by submicrometer-sized fluidic channels. Anal Chem 76(6):1618–26.

Förster T. 1948. Intramolecular energy migration and fluorescence. Ann Physik 2:55–75.

Funatsu T, Harada Y, Tokunaga M, Saito K, Yanagida T. 1995. Imaging of single fluorescent molecules and individual ATP turnovers by single myosin molecules in aqueous solution. Nature 374(6522):555–9.

Goodman RP, Berry RM, Turberfield AJ. 2004. The single-step synthesis of a DNA tetrahedron. Chem Commun (Cambridge) 12:1372–3.

Goodman RP, Heilemannt M, Dooset S, Erben CM, Kapanidis AN, Turberfield AJ. 2008. Reconfigurable, braced, three-dimensional DNA nanostructures. Nat Nanotechnol 3(2):93–96.

Goodman RP, Schaap IA, Tardin CF, Erben CM, Berry RM, Schmidt CF, Turberfield AJ. 2005. Rapid chiral assembly of rigid DNA building blocks for molecular nanofabrication. Science 310(5754):1661–5.

Greenleaf WJ, Woodside MT, Block SM. 2007. High-resolution, single-molecule measurements of biomolecular motion. Annu Rev Biophys Biomol Struct 36:171–90.

Guo J, Xu N, Li Z, Zhang S, Wu J, Kim DH, Sano Marma M, Meng Q, Cao H, Li X, et al. 2008. Four-color DNA sequencing with 3'-O-modified nucleotide reversible terminators and chemically cleavable fluorescent dideoxynucleotides. Proc Nat Acad Sci USA 105(27):9145–50.

Ha T. 2001. Single-molecule fluorescence resonance energy transfer. Methods 25:78–86.

Ha T. 2004. Structural dynamics and processing of nucleic acids revealed by single-molecule spectroscopy. Biochemistry 43(14):4055–63.

Ha T, Enderle T, Ogletree DF, Chemla DS, Selvin PR, Weiss S. 1996. Probing the interaction between two single molecules: fluorescence resonance energy transfer between a single donor and a single acceptor. Proc Natl Acad Sci USA 93(13):6264–8.

Ha T, Rasnik I, Cheng W, Babcock HP, Gauss GH, Lohman TM, Chu S. 2002. Initiation and re-initiation of DNA unwinding by the *Escherichia coli* Rep helicase. Nature 419(6907):638–41.

Ha T, Ting AY, Liang J, Caldwell WB, Deniz AA, Chemla DS, Schultz PG, Weiss S. 1999a. Single-molecule fluorescence spectroscopy of enzyme conformational dynamics and cleavage mechanism. Proc Natl Acad Sci USA 96(3):893–8.

Ha T, Ting AY, Liang J, Deniz AA, Chemla DS, Schultz PG, Weiss S. 1999b. Temporal fluctuations of fluorescence resonance energy transfer between two dyes conjugated to a single protein. Chem Phys 247:107–118.

Ha T, Zhuang X, Kim HD, Orr JW, Williamson JR, Chu S. 1999c. Ligand-induced conformational changes observed in single RNA molecules. Proc Natl Acad Sci USA 96(16):9077–82.

Haas E, Katchalski-Katzir E, Steinberg IZ. 1978. Effect of the orientation of donor and acceptor on the probability of energy transfer involving electronic transitions of mixed polarization. Biochemistry 17(23):5064–70.

Haas E, Wilchek M, Katchalski-Katzir E, Steinberg IZ. 1975. Distribution of end-to-end distances of oligopeptides in solution as estimated by energy transfer. Proc Natl Acad Sci USA 72(5):1807–11.

Harms GS, Orr G, Montal M, Thrall BD, Colson SD, Lu HP. 2003. Probing conformational changes of gramicidin ion channels by single-molecule patch-clamp fluorescence microscopy. Biophys J 85(3):1826–38.

Harris TD, Buzby PR, Babcock H, Beer E, Bowers J, Braslavsky I, Causey M, Colonell J, Dimeo J, Efcavitch JW, et al. 2008. Single-molecule DNA sequencing of a viral genome. Science 320(5872):106–9.

Heilemann M, Tinnefeld P, Sanchez Mosteiro G, Garcia Parajo M, Van Hulst NF, Sauer M. 2004. Multistep energy transfer in single molecular photonic wires. J Am Chem Soc 126(21):6514–5.

Henzler-Wildman KA, Thai V, Lei M, Ott M, Wolf-Watz M, Fenn T, Pozharski E, Wilson MA, Petsko GA, Karplus M, et al. 2007. Intrinsic motions along an enzymatic reaction trajectory. Nature 450(7171):838–44.

Herbert KM, Greenleaf WJ, Block SM. 2008. Single-molecule studies of RNA polymerase: motoring along. Annu Rev Biochem 77:149–76.

Hohng S, Joo C, Ha T. 2004. Single-molecule three-color FRET. Biophys J 87(2):1328–37.

Hohng S, Zhou RB, Nahas MK, Yu J, Schulten K, Lilley DMJ, Ha TJ. 2007. Fluorescence-force spectroscopy maps two-dimensional reaction landscape of the Holliday junction. Science 318(5848):279–83.

Jares-Erijman EA, Jovin TM. 2003. FRET imaging. Nat Biotechnol 21(11):1387–95.

Joo C, McKinney SA, Nakamura M, Rasnik I, Myong S, Ha T. 2006. Real-time observation of RecA filament dynamics with single monomer resolution. Cell 126(3):515–27.

Kapanidis AN, Ebright YW, Ebright RH. 2001. Site-specific incorporation of fluorescent probes into protein: hexahistidine-tag-mediated fluorescent labeling with (Ni(2+):nitrilotriacetic acid (n)-fluorochrome conjugates. J Am Chem Soc 123(48):12123–5.

Kapanidis AN, Lee NK, Laurence TA, Doose S, Margeat E, Weiss S. 2004. Fluorescence-aided molecule sorting: analysis of structure and interactions by alternating-laser excitation of single molecules. Proc Natl Acad Sci USA 101(24):8936–41.

Kapanidis AN, Margeat E, Ho SO, Kortkhonjia E, Weiss S, Ebright RH. 2006. Initial transcription by RNA polymerase proceeds through a DNA-scrunching mechanism. Science 314(5802):1144–7.

Kapanidis AN, Margeat E, Laurence TA, Doose S, Ho SO, Mukhopadhyay J, Kortkhonjia E, Mekler V, Ebright RH, Weiss S. 2005. Retention of transcription initiation factor sigma(70) in transcription elongation: single-molecule analysis. Mol Cell 20(3):347–56.

Kapanidis AN, Weiss S. 2002. Fluorescent probes and bioconjugation chemistries for single-molecule fluorescence analysis of biomolecules. J Chem Phys 117(24):10953–64.

Karymov M, Chinnaraj M, Bogdanov A, Srinivasan AR, Zheng G, Olson WK, Lyubchenko Y. 2008a. Structure, dynamics, and branch migration of a DNA Holliday junction: a single-molecule fluorescence and modeling study. Biophys J. 95(9):4372–83

Karymov M, Daniel D, Sankey OF, Lyubchenko YL. 2005. Holliday junction dynamics and branch migration: single-molecule analysis. Proc Natl Acad Sci USA 102(23):8186–91.

Karymov MA, Bogdanov A, Lyubchenko YL. 2008b. Single molecule fluorescence analysis of branch migration of Holliday junctions: effect of DNA sequence. Biophys J 95(3):1239–47.

Koopmans WJ, Brehm A, Logie C, Schmidt T, van Noort J. 2007. Single-pair FRET microscopy reveals mononucleosome dynamics. J Fluoresc 17(6):785–95.

Kuzmenkina EV, Heyes CD, Nienhaus GU. 2005. Single-molecule Forster resonance energy transfer study of protein dynamics under denaturing conditions. Proc Natl Acad Sci USA 102(43):15471–6.

Lakowicz JR. 2006. *Principles of Fluorescence Spectroscopy*, 3rd ed. Springer, New York.

Lang MJ, Fordyce PM, Block SM. 2003. Combined optical trapping and single-molecule fluorescence. J Biol 2(1):6.

Laurence TA, Kong XX, Jager M, Weiss S. 2005. Probing structural heterogeneities and fluctuations of nucleic acids and denatured proteins. Proc Natl Acad Sci USA 102(48):17348–53.

Lee NK, Kapanidis AN, Koh HR, Korlann Y, Ho SO, Kim Y, Gassman N, Kim SK, Weiss S. 2007. Three-color alternating-laser excitation of single molecules: monitoring multiple interactions and distances. Biophys J 92(1):303–12.

Lee NK, Kapanidis AN, Wang Y, Michalet X, Mukhopadhyay J, Ebright RH, Weiss S. 2005. Accurate FRET measurements within single diffusing biomolecules using alternating-laser excitation. Biophys J 88(4):2939–53.

Levene MJ, Korlach J, Turner SW, Foquet M, Craighead HG, Webb WW. 2003. Zero-mode waveguides for single-molecule analysis at high concentrations. Science 299(5607):682–6.

Lipman EA, Schuler B, Bakajin O, Eaton WA. 2003. Single-molecule measurement of protein folding kinetics. Science 301(5637):1233–5.

Lippincott-Schwartz J, Snapp E, Kenworthy A. 2001. Studying protein dynamics in living cells. Nat Rev Mol Cell Biol 2(6):444–56.

Margeat E, Kapanidis AN, Tinnefeld P, Wang Y, Mukhopadhyay J, Ebright RH, Weiss S. 2006. Direct observation of abortive initiation and promoter escape within single immobilized transcription complexes. Biophys J 90(4):1419–31.

Margittai M, Widengren J, Schweinberger E, Schroder GF, Felekyan S, Haustein E, Konig M, Fasshauer D, Grubmuller H, Jahn R, et al. 2003. Single-molecule fluorescence resonance energy transfer reveals a dynamic equilibrium between closed and open conformations of syntaxin 1. Proc Natl Acad Sci USA 100(26): 15516–21.

McKinney SA, Declais AC, Lilley DM, Ha T. 2003. Structural dynamics of individual Holliday junctions. Nat Struct Biol 10(2):93–7.

McKinney SA, Freeman AD, Lilley DM, Ha T. 2005. Observing spontaneous branch migration of Holiday junctions one step at a time. Proc Natl Acad Sci USA. 102(16):5715–5720.

McKinney SA, Joo C, Ha T. 2006. Analysis of single-molecule FRET trajectories using hidden Markov modeling. Biophys J 91(5):1941–51.

Michalet X, Pinaud FF, Bentolila LA, Tsay JM, Doose S, Li JJ, Sundaresan G, Wu AM, Gambhir SS, Weiss S. 2005. Quantum dots for live cells, in vivo imaging, and diagnostics. Science 307(5709):538–44.

Michalet X, Weiss S, Jager M. 2006. Single-molecule fluorescence studies of protein folding and conformational dynamics. Chem Rev 106(5):1785–813.

Miyawaki A, Tsien RY. 2000. Monitoring protein conformations and interactions by fluorescence resonance energy transfer between mutants of green fluorescent protein. Appl Chimeric Genes Hybrid Proteins B 327:472–500.

Moerner WE, Fromm DP. 2003. Methods of single-molecule fluorescence spectroscopy and microscopy. Rev Sci Instrum 74(8):3597–619.

Morgan MA, Okamoto K, Kahn JD, English DS. 2005. Single-molecule spectroscopic determination of lac repressor-DNA loop conformation. Biophys J 89(4):2588–96.

Mori T, Vale RD, Tomishige M. 2007. How kinesin waits between steps. Nature 450(7170):750–4.

Muller BK, Reuter A, Simmel FC, Lamb DC. 2006. Single-pair FRET characterization of DNA tweezers. Nano Lett 6(12):2814–20.

Muller BK, Zaychikov E, Brauchle C, Lamb DC. 2005. Pulsed interleaved excitation. Biophys J 89(5):3508–522.

Murakoshi H, Iino R, Kobayashi T, Fujiwara T, Ohshima C, Yoshimura A, Kusumi A. 2004. Single-molecule imaging analysis of Ras activation in living cells. Proc Natl Acad Sci USA 101(19):7317–22.

Myong S, Bruno MM, Pyle AM, Ha T. 2007. Spring-loaded mechanism of DNA unwinding by hepatitis C virus NS3 helicase. Science 3l7(5837):513–6.

Myong S, Rasnik I, Joo C, Lohman TM, Ha T. 2005. Repetitive shuttling of a motor protein on DNA. Nature 437(7063):1321–5.

Nie S, Chiu DT, Zare RN. 1994. Probing individual molecules with confocal fluorescence microscopy. Science 266(5187):1018–21.

Noji H, Yasuda R, Yoshida M, Kinosita K, Jr. 1997. Direct observation of the rotation of F1-ATPase. Nature 386(6622):299–302.

Rasnik I, McKinney SA, Ha T. 2006. Nonblinking and longlasting single-molecule fluorescence imaging. Nat Methods 3(11):891–3.

Rasnik I, Myong S, Cheng W, Lohman TM, Ha T. 2004. DNA-binding orientation and domain conformation of the E. coli rep helicase monomer bound to a partial duplex junction: single-molecule studies of fluorescently labeled enzymes. J Mol Biol 336(2):395–408.

Rhoades E, Gussakovsky E, Haran G. 2003. Watching proteins fold one molecule at a time. Proc Nat Acad Sci USA 100(6):3197–202.

Rice S, Lin AW, Safer D, Hart CL, Naber N, Carragher BO, Cain SM, Pechatnikova E, Wilson-Kubalek EM, Whittaker M, et al. 1999. A structural change in the kinesin motor protein that drives motility. Nature 402(6763): 778–84.

Ross J, Buschkamp P, Fetting D, Donnermeyer A, Roth CM, Tinnefeld P. 2007. Multicolor single-molecule spectroscopy with alternating laser excitation for the investigation of interactions and dynamics. J Phys Chem B 111(2):321–6.

Rothemund PW. 2006. Folding DNA to create nanoscale shapes and patterns. Nature 440(7082):297–302.

Rothwell PJ, Berger S, Kensch O, Felekyan S, Antonik M, Wohrl BM, Restle T, Goody RS, Seidel CA. 2003. Multiparameter single-molecule fluorescence spectroscopy reveals heterogeneity of HIV-1 reverse transcriptase:primer/template complexes. Proc Natl Acad Sci USA 100(4):1655–60.

Sabanayagam CR, Eid JS, Meller A. 2004. High-throughput scanning confocal microscopy for single molecule analysis. Appl Phys Lett 84(7):1216–8.

Sako Y, Minoghchi S, Yanagida T. 2000. Single-molecule imaging of EGFR signalling on the surface of living cells. Nat Cell Biol 2(3):168–72.

Sapsford KE, Berti L, Medintz IL. 2006. Materials for fluorescence resonance energy transfer analysis: beyond traditional donor-acceptor combinations. Angew Chem Int Ed 45(28):4562–88.

Schluesche P, Stelzer G, Piaia E, Lamb DC, Meisterernst M. 2007. NC2 mobilizes TBP on core promoter TATA boxes. Nat Struct Mol Biol 14(12):1196–201.

Schuler B, Eaton WA. 2008. Protein folding studied by single-molecule FRET. Curr Opin Struct Biol 18(1):16–26.

Schuler B, Lipman EA, Eaton WA. 2002. Probing the free-energy surface for protein folding with single-molecule fluorescence spectroscopy. Nature 419(6908):743–7.

Seeman NC. 2003. DNA in a material world. Nature 421(6921):427–31.

Seeman NC. 2005. From genes to machines: DNA nanomechanical devices. Trends Biochem Sci 30(3):119–25.

Selvin PR. 1995. Fluorescence resonance energy transfer. Methods Enzymol 246:300–34.

Selvin PR. 2000. The renaissance of fluorescence resonance energy transfer. Nat Struct Biol 7(9):730–4.

Sharma S, Chakraborty K, Muller BK, Astola N, Tang YC, Lamb DC, Hayer-Hartl M, Hartl FU. 2008. Monitoring protein conformation along the pathway of chaperonin-assisted folding. Cell 133(1):142–53.

Shroff H, Reinhard BM, Siu M, Agarwal H, Spakowitz A, Liphardt J. 2005. Biocompatible force sensor with optical readout and dimensions of 6 nm(3). Nano Lett 5(7):1509–14.

Smiley RD, Collins TR, Hammes GG, Hsieh TS. 2007. Single-molecule measurements of the opening and closing of the DNA gate by eukaryotic topoisomerase II. Proc Natl Acad Sci USA 104(12):4840–5.

Stryer L, Haugland RP. 1967. Energy transfer: a spectroscopic ruler. Proc Natl Acad Sci USA 58(2):719–26.

Talaga DS, Lau WL, Roder H, Tang J, Jia Y, DeGrado WF, Hochstrasser RM. 2000. Dynamics and folding of single two-stranded coiled-coil peptides studied by fluorescent energy transfer confocal microscopy. Proc Natl Acad Sci USA 97(24):13021–6.

Tan E, Wilson TJ, Nahas MK, Clegg RM, Lilley DM, Ha T. 2003. A four-way junction accelerates hairpin ribozyme folding via a discrete intermediate. Proc Natl Acad Sci USA 100(16):9308–13.

Tarsa PB, Brau RR, Barch M, Ferrer JM, Freyzon Y, Matsudaira P, Lang MJ. 2007. Combined optical tweezers force measurement with simultaneous single molecule fluorescence resonance energy transfer (FRET) detection. Biophys J 654A.

Tomishige M, Stuurman N, Vale RD. 2006. Single-molecule observations of neck linker conformational changes in the kinesin motor protein. Nat Struct Mol Biol 13(10):887–94.

Vale RD. 2003. The molecular motor toolbox for intracellular transport. Cell 112(4):467–80.

Vogelsang J, Doose S, Sauer M, Tinnefeld P. 2007. Single-molecule fluorescence resonance energy transfer in nanopipets: improving distance resolution and concentration range. Anal Chem 79(19):7367–75.

Vogelsang J, Kasper R, Steinhauer C, Person B, Heilemann M, Sauer M, Tinnefeld P. 2008. A reducing and oxidizing system minimizes photobleaching and blinking of fluorescent dyes. Angew Chem Int Ed Engl 47(29):5465–9.

Walter NG, Huang CY, Manzo AJ, Sobhy MA. 2008. Do-it-yourself guide: how to use the modern single-molecule toolkit. Nat Methods 5(6):475–89.

Webb SE, Roberts SK, Needham SR, Tynan CJ, Rolfe DJ, Winn MD, Clarke DT, Barraclough R, Martin-Fernandez ML. 2008. Single-molecule imaging and fluorescence lifetime imaging microscopy show different structures for high- and low-affinity epidermal growth factor receptors in A431 cells. Biophys J 94(3):803–19.

Weiss S. 1999. Fluorescence spectroscopy of single biomolecules. Science 283(5408):1676–83.

Weiss S. 2000. Measuring conformational dynamics of biomolecules by single molecule fluorescence spectroscopy. Nat Struct Biol 7(9):724–9.

Wu P, Brand L. 1994. Resonance energy transfer: methods and applications. Anal Biochem 218(1):1–13.

Wu PG, Brand L. 1992. Orientation factor in steady-state and time-resolved resonance energy-transfer measurements. Biochemistry 31(34):7939–47.

Yildiz A, Tomishige M, Vale RD, Selvin PR. 2004. Kinesin walks hand-over-hand. Science 303(5658):676–8.

Yurke B, Turberfield AJ, Mills AP, Jr., Simmel FC, Neumann JL. 2000. A DNA-fuelled molecular machine made of DNA. Nature 406(6796):605–8.

Zhuang X, Bartley LE, Babcock HP, Russell R, Ha T, Herschlag D, Chu S. 2000. A single-molecule study of RNA catalysis and folding. Science 288(5473):2048–51.

Zhuang X, Kim H, Pereira MJ, Babcock HP, Walter NG, Chu S. 2002. Correlating structural dynamics and function in single ribozyme molecules. Science 296(5572):1473–6.

Zhuang X, Rief M. 2003. Single-molecule folding. Curr Opin Struct Biol 13(1):88–97.

Zimmer M. 2002. Green fluorescent protein (GFP): applications, structure, and related photophysical behavior. Chem Rev 102(3):759–81.

Zimmermann B, Diez M, Borsch M, Graber P. 2006. Subunit movements in membrane-integrated EF0F1 during ATP synthesis detected by single-molecule spectroscopy. Biochim Biophys Acta 1757(5–6):311–9.